Journal of Environmental Management 393 (2025) 126955

Contents lists available at ScienceDirect

Journal of Environmental Management

journal homepage: www.elsevier.com/locate/jenvman

Research article

Drivers of anoxia in a eutrophic lagoon with clams farming (Sacca di Goro Lagoon, Italy): risk evaluation via multivariate statistics and timescales analysis

Diana M. Arroyave Gómez [a,*], Leonardo Morini [b], Samuele Pagani [a,b,c], Sara Benelli [a], Monia Magri [a], Georg Umgiesser [d,e], Luis Germano Biolchi [f], Giuseppe Castaldelli [b], Marco Bartoli [a]

[a] Department of Chemistry, Life Sciences and Environmental Sustainability, University of Parma, Italy
[b] Department of Department of Environmental and Prevention Sciences, University of Ferrara, Italy
[c] International Marine Centre - IMC Foundation, Loc. Sa Mardini, Torregrande, Oristano, 09170, Italy
[d] Institute of Marine Sciences – National Research Council (ISMAR-CNR), Venice, Italy
[e] Institute of Marine Research, Klaipeda University, Klaipeda, Lithuania
[f] Hydro-Meteo-Climate Service of the Regional Agency for Prevention, Environment and Energy of Emilia-Romagna, Arpae-SIMC, Italy

ARTICLE INFO

Keywords:
Clam aquaculture
Stable isotopes
Benthic turnover
Benthic–pelagic coupling
Transport timescales

ABSTRACT

The anoxia risk in a shallow coastal lagoon (Sacca di Goro (SG), Italy) experiencing multiple pressures (clam aquaculture, anthropogenic nutrient inputs, climate change) was assessed by combining timescales of anoxia onset, benthic nutrient turnover, horizontal and vertical transport, multivariate statistics, and Geographic Information System (GIS). The biogeochemical and transport timescales were obtained by experimental measurements and physical modeling. To this purpose, daily oxygen (O_2) and nutrient fluxes [dissolved inorganic phosphorus (DIP), ammonium (NH_4^+), dissolved reactive silica (SiO_2)] were measured in the benthic and pelagic compartments at six areas of the lagoon catching its complex spatial heterogeneity due to riverine and marine inputs, clams farming, depths, flushing and vertical exchange times, amount and quality of organic matter. Water quality, sedimentary features and fluxes and pore water chemistry were also measured. This approach allowed us to estimate the contribution of the benthic and pelagic compartments to the onset of anoxia, as well as to determine the main drivers that may lead to anoxia. The results show that the anoxia onset in the SG is mainly determined by the clam biomass. This is due to shorter timescales of both anoxia onset and benthic nutrient turnover times (faster rates of O_2 consumption and nutrient replenishment) in farming than in non-farming areas. However, the anoxia onset in the deepest part of the lagoon is also favored by water column respiration. On the other hand, vertical exchange times shorter than flushing times suggest that vertical mixing is the dominant physical factor in controlling the O_2 replenishment in the SG lagoon, counteracting the anoxia risk. The timescales analysis is a simple and effective method to understand the interplay between O_2 consumption and physical processes in a complex shallow eutrophic lagoon, which is a key issue in the environmental management of coastal lagoons farmed areas.

1. Introduction

Bivalve farming (e.g., mussels, oysters and clams) has undergone rapid expansion over recent decades in diverse coastal ecosystems around the world (e.g., lagoons, coastal bays, offshore areas) (Newton et al., 2014). In Europe, more than 90 % of seafood production consists of bivalve mollusks, mainly farmed in shallow and semi-enclosed coastal lagoons (Newton et al., 2014). This fast-growing global industry poses concerns with respect to its environmental impact and long-term ecological and economic sustainability (Marinov et al., 2007).

Bivalves displace pelagic primary production to the sediment via filtration and biodeposition of feces and pseudofeces and favor nutrient recycling via excretion, linking benthic and pelagic compartments (Nizzoli et al., 2007; Newton et al., 2014; Nicholaus and Zheng, 2014).

* Corresponding author.
E-mail address: dianamarcela.arroyavegomez@unipr.it (D.M. Arroyave Gómez).

https://doi.org/10.1016/j.jenvman.2025.126955
Received 18 November 2024; Received in revised form 22 July 2025; Accepted 10 August 2025
Available online 20 August 2025

The whole system relevance of mollusks-mediated biogeochemical processes depends on the standing stock of farmed organisms (Melià et al., 2003). Farmed mollusks can impact ecosystem functioning due to large inputs of labile biodeposits, stimulating anaerobic metabolism and nutrient recycling, which enhance algal growth and collapse, and dystrophic conditions (Bartoli et al., 2001; Viaroli et al., 2006; Lacoste et al., 2022; Le Ray et al., 2023). Such impacts interact with other pressures (e.g., anthropogenic pollution, global warming) and decrease dissolved oxygen (DO) availability, with cascade consequences for aerobic organisms and biogeochemical cycles (Meire et al., 2013; Gammal et al., 2017; Schmidt et al., 2017). The dropping of DO concentrations in the water column to hypoxia (<2 mg $O_2 \cdot L^{-1}$) and anoxia (0 mg $O_2 \cdot L^{-1}$) levels is a global key stressor, affecting estuarine and marine benthic ecosystem functioning worldwide, and a wide variety of ecological and economic services (Diaz and Rosenberg, 2008; Peña et al., 2010; Breitburg et al., 2018). Low DO levels are generally attributed to the synergy between anthropogenic pressures and hydro-climatic forcings (Derolez et al., 2020; Le Ray et al., 2023). These pressures are predicted to increase in magnitude, duration and extension in the coming decades due to ongoing human-induced eutrophication and global warming (e.g., higher frequency of extreme climatic events such as summer heat waves or strong riverine outflows), potentially affecting sea-based economic sectors such as mollusks aquaculture (Villnäs et al., 2012; Rodrigues et al., 2015; Le Ray et al., 2023).

The DO concentration depends on a tight balance between its physical inputs (e.g., water mass transport and mixing, water-atmosphere exchanges), biological production (e.g., photosynthesis), and its removal processes, such as biological respiration, nitrification, oxidation of reduced chemical species (e.g., manganese (Mn[II]), iron (Fe[II]), free sulphides ($H_2S = \sum H_2S + HS^- + S^{2-}$)), and outgassing across the air–sea interface (Zhang et al., 2010; Fennel and Testa, 2019). The excessive inputs of anthropogenic nutrients induce high DO consumption, resulting from organic matter mineralization in surface sediments. Sediments can account for up to 80 % of the total O_2 consumption in shallow coastal systems (Seitaj et al., 2017); this O_2 sink can be further strengthened by other factors such as long residence time of the water, along with reduced horizontal advection and/or reduced vertical mixing due to stratification (Fennel and Testa, 2019; Rigaud et al., 2021; Pittaluga et al., 2022). The increase in water residence time enhances nutrients retention within the system, reinforcing the relative importance of several internal biogeochemical processes (e.g., recycling of bioavailable nutrients) (Mosley et al., 2023). On the other hand, in mollusks farming areas, filter-feeding bivalves superimpose and interact with physical, chemical and biological factors that contribute to the O_2 balance (Viaroli et al., 2006; Lavoie et al., 2016). High densities of burrowing mollusks as clams increase sediment respiration rates, excretion of nitrogenous compounds, and the enrichment of the sediment with organic matter via labile biodeposits (Bartoli et al., 2001). Therefore, the accumulation and excess of both natural and anthropogenic organic matter in the proximity of mollusks farms rapidly depletes DO to anoxic levels in superficial sediments, causing a shift from aerobic respiration to a predominance of anaerobic respiration pathways, such as sulfate reduction. However, clams can also contribute to sediment oxygenation through bioturbation activities (bioirrigation and biomixing) (Nizzoli et al., 2006; Nicholaus and Zheng, 2014).

The formation of hypoxia/anoxia is highly dynamic, and may vary in extent, severity and frequency (Villnäs et al., 2012). Assessing and managing the risk of hypoxia/anoxia in mollusk farms is complex, due to the effect of diverse forcing of site-specific factors (e.g., mollusk species and rearing densities, anthropogenic pollution sources, organic matter amount and quality, water column stratification and physical transport processes, climate patterns and variability, etc.) acting over a wide range of temporal and spatial scales (Marinov et al., 2008; Lavoie et al., 2016; Lacoste et al., 2022; Le Ray et al., 2023). Additionally, DO availability in both pelagic and benthic compartments is tightly interconnected. The identification of the factors that influence DO availability remains challenging, with the aim to better understand the duration, intensity, and frequency of hypoxia/anoxia events and their consequences on benthic-pelagic coupling in coastal ecosystems (Rigaud et al., 2021).

Hypoxia/anoxia risk has been studied using both experimental (e.g., sediment incubation) and a variety of modeling approaches (e.g., DO budgeting, hydrodynamic-biogeochemical models, indeces, timescales methods) (Melià et al., 2003; Druon et al., 2004; Marinov et al., 2008; Shen et al., 2013; Groβe et al., 2016; Fennel and Testa, 2019; Leoni et al., 2022; Rigaud et al., 2021; Le Ray et al., 2023; Shen and Qin, 2024). Timescale methods are useful in simplifying, understanding and modeling complex coastal aquatic ecosystems, as they have the same units with which the speed of disparate processes can be compared. For instance, the use of both biogeochemical timescales (e.g., nutrients benthic turnover, consumption, etc.) and transport timescales (e.g., residence time, flushing time, and/or vertical exchange time) can help to understand the coupled physical-biogeochemical systems (Lucas and Deleersnijder, 2020).

The Sacca di Goro (SG) Lagoon is one of the most important European sites for clam (*Ruditapes philippinarum*) farming, with an annual production that reached a maximum of approximately 15,000 t $year^{-1}$ in the early 1990s (Marinov et al., 2007). Summer dystrophic events occurred since the late 80's causing massive mortalities of clam stocks, which limited the annual production to about 10,000 t (Vincenzi et al., 2006). Dystrophic crises were mainly attributed to the proliferation of the green seaweed *Ulva rigida* and water stagnation in some areas of the lagoon (Melià et al., 2003; Viaroli et al., 2006; Marinov et al., 2008). Despite interventions to improve water circulation and reduce algal growth, the SG remains at high risk of undergoing anoxia events. The SG thereby provides an excellent, complex and challenging system to analyze the contribution and changes of several drivers that have led and may still lead to anoxia events.

This work aims at improving our understanding of the physical, chemical and biological drivers in both pelagic and benthic compartments that contribute to anoxia risk in this shallow lagoon devoted to clam aquaculture. To this purpose, a detailed quantification and analysis of biogeochemical processes (i.e., anoxia onset and nutrient benthic turnover times) and physical processes modeling (i.e., flushing time and vertical mixing) was conducted across different timescales. Experimental work also included measurements of sedimentary features, porewater and water quality parameters. To identify different patterns and extract useful information or/and knowledge for decision-makers regarding anoxia risk management in the SG, we applied a combined analysis of timescales/multivariate analysis/Geographic Information System (GIS). We hypothesized that two main interacting factors contribute to the risk of anoxia in the SG. The first factor is the clam biomass, as higher biomass results in greater benthic respiration and excretion rates. The second factor is the physical transport process (vertical or horizontal) that dominates DO replenishment, as transport timescales larger than O_2 consumption can dramatically increase the anoxia risk.

2. Materials and methods

2.1. Description of the study area

The SG is a shallow and semi-enclosed coastal lagoon located in the southern part of the Po River Delta in the province of Ferrara, Italy. The SG has a triangular shape with superficial area of about 27 Km^2, is delimited by the Po di Goro River, the southernmost branch of the Po River, and is partially separated from the Adriatic Sea by two spits, the Scanno di Goro and the Scanno di Volano (Fig. 1) (Maicu et al., 2021). The lagoon has an average depth of 1.5 m, a water volume of 39×10^6 m^3 and water retention times ranging from 1 to 4 days (Viaroli et al., 2006; Marinov et al., 2007). Most of the lagoon surface (87 %) consists of tidal flats (Maicu et al., 2018). The SG has freshwater inputs, mainly from the Po di Volano River in the western area and from the Po di Goro

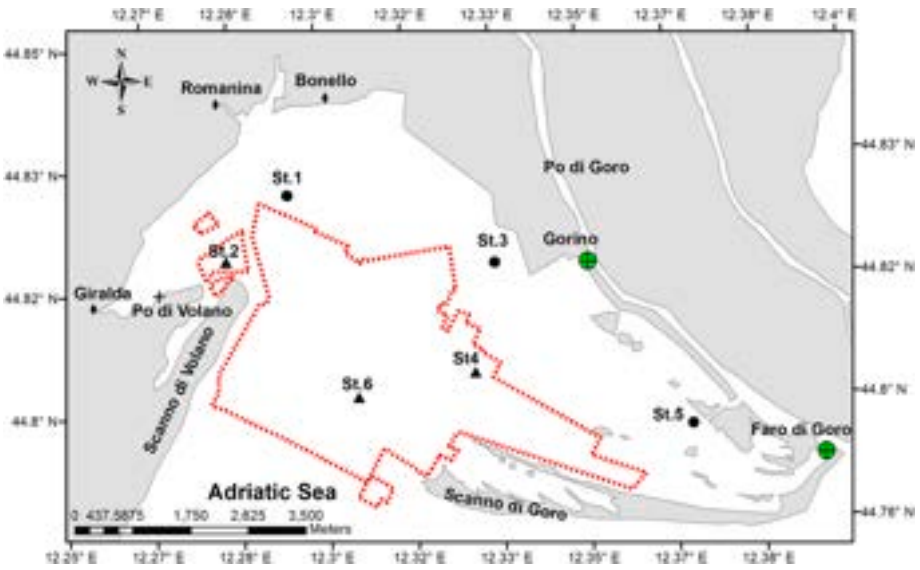

Fig. 1. Location of clam farming area in the Sacca di Goro (SG) Lagoon, including its main freshwater tributaries (Po di Volano River, Giralda, Romania and Bonello channels, and Gorino and Faro di Goro locks) and the stations sampled during summer 2023. The red dotted line indicates the exploited area of the lagoon for clam farming. The spatial distribution of the selected stations considered clams farmed (St.2, St.4 and St.6) and non-farmed areas (St.1, St.3 and St.5).

River along the eastern zone. The main connections with the Po di Goro River are the Gorino and Faro di Goro locks, which are manually managed by the local authorities to ensure the most favorable salinity and nutrient conditions for the lagoon productivity. These gates are opened during the summer to enhance the water renewal, and are closed during the river floods to ensure an acceptable salinity in the lagoon and prevent sediment deposition (Maicu et al., 2021). Pumping stations (Romanina, Giralda, Bonello) also provide lower freshwater inputs to the lagoon (Fig. 1).

Bottom sediments of the SG are composed of typical alluvial mud with high clay and silt deposits in the northern and central zones. Sandy sediments characterize the lagoon's mouth, whilst muddy sediments are common in the eastern corner (Viaroli et al., 2006; Zilius et al., 2015).

2.2. Sampling strategy to assess the anoxia risk in the SG lagoon

Water and sediment sampling was carried out at six stations: St.1, St.3 and St.5, which are located in non-clams farming area, and St.2, St.4 and St.6, located in the clam farming area. Stations spatial distribution also considered the influence of riverine and channels inputs (St.1, St.2 and St.5) and marine water (St.3, St.4 and St.6), as well as the depth, distinguishing between shallow stations (St.1, St.2, St.4, St.5 and St.6) and a relatively deep area represented by St.3 (Fig. 1 and Table 1S).

Water quality and sediment cores samplings were carried out during three field campaigns on June 27th, 2023 (St.1 and St.2), July 3rd, 2023 (St.3 and St.4) and July 11th, 2023 (St.5 and St.6) (Fig. 1 and Table 1S). In each field campaign, a station without and one with clams were sampled. Water quality parameters, including water temperature, salinity, DO and pH were measured in situ with a multiparameter probe (YSI Instruments, Mod. 556). Integrated water samples (n = 6) were collected at each station with a PVC pipe (i.d. 2 cm, length 2 m). Subsamples were filtered for nutrients (Whatman GF/F glass fiber filters) and chlorophyll-a (Chl-a, Whatman GF/F glass fiber filters), and frozen for later measurements (Table 1). Ammonium (NH_4^+) was determined by indophenol method, nitrite (NO_2^-) by sulfanilamide, nitrate (NO_3^-) by cadmium reduction, dissolved inorganic phosphorus (DIP) by ascorbic acid method and dissolved reactive silica (SiO_2) by molybdate method (APHA, 2012). The Chl-a was extracted with 90 % acetone and determined spectrophotometrically (Lorenzen, 1967). The Dissolved Inorganic Nitrogen (DIN) was calculated as $DIN = NH_4^+ + NO_2^- + NO_3^-$.

The sediment cores sampling was conducted immediately after the water quality sampling at each station. Transparent Plexiglas liners (i.d. 8 cm, length 30 cm, n = 6 per station) were used for benthic O_2 and nutrient flux measurements, while smaller liners (i.d. 4 cm, length 20 cm, n = 6 per station) were used for sediment features measurements. At the deeper sites, muddy sediments were collected using a hand-corer, whereas at sandy shallower sites, they were collected by hand. All cores had approximately equal heights of sediment and overlying water column. Once collected, the cores were bottom and top capped and brought to the boat where the top lid was removed, and the cores were submerged in a tank containing in-situ water cooled with ice packs. Bottom water (~150 L) was also collected from each site for core

Table 1
Summary of experimental activities carried out at each station for benthic and pelagic compartments in the Sacca di Goro (SG) Lagoon during summer 2023.

Measurement	Sampling design	Parameters	Methods
Water quality	Sampling in water column	Temperature, salinity and OD_{WC} DIP_{WC}, NH_{4wc}^+, NO_{3wc}^-, DIN_{WC}, $SiO_{2\ wc}$ and Chl-a wc.	Multiparameter probe Spectrophotometry
Benthic incubations	Dark and light incubation. Large cores	O_{2Bc} DIP_{Bc}, NH_{Bc}^+ and SiO_{2Bc}	O_2 microsensor Spectrophotometry
		Clam biomass (flesh dry weight)	Gravimetric
Water incubations	Dark and light incubation. Small cores	O_{2Pg} DIP_{Pg}, NH_{Pg}^+ and SiO_{2pg}	O_2 microsensor Spectrophotometry
Water incubations with algae (*Ulva* sp., and *Gracilaria* sp.)	Dark and light incubation. Small cores	O_2	O_2 microsensor
Pore water extraction	0–4 cm layer with Rhizon™ samplers. Large cores	NH_{4pw}^+, DIP_{pw}, SiO_{2pw} and H_2S_{pw}, $Mn_{pw}(II)$ and $Fe_{pw}(II)$	Spectrophotometry Atomic absorption
Sediment features	0–4 cm superficial layer. Small cores	Chl-a_{Sed} (0–1 cm) Fe_{tot} and %Fe $(III)_{sed}$ (0–4 cm)	Spectrophotometry Spectrophotometry
		TOC, TN, $\delta^{13}C$ and $\delta^{15}N$ (0–4 cm)	Mass spectrometry

maintenance, preincubation and incubation. Cores and bottom water were transported to the laboratory within 3 h from retrieval. The water inside the cores was gently stirred by a Teflon - coated magnetic bar driven by an external motor rotating at 40 rpm, avoiding sediment resuspension. During overnight preincubation, the cores were maintained submersed with the top open and the stirring on. The water in the tanks (one tank per station) was maintained at in situ conditions and at 100 % O_2 saturation using aquarium pumps and aerators.

During sampling, algae (*Ulva* sp., and *Gracilaria* sp.) were only present at the St.6. Both algal genera were randomly sampled through a plastic square frame (30 × 30 cm) that was randomly thrown (n = 6) onto the sediment surface. Algae inside the frame were collected, separated, drained and weighed fresh to estimate in situ biomass of each algal genus. This provided reference values for the amounts to be added to seaweed incubations.

2.3. Measurements of benthic and pelagic fluxes in areas with and without clams in the SG lagoon

The day after sampling, the water in the tanks was exchanged with new water from each station. The dark incubations were carried out first, followed by a 2 h light preincubation period, before starting the light incubations. Irradiance at the sediment surface was set to reproduce the daily average irradiance of the sampling period (180 ± 60 μE m^{-2} s^{-1}). This value was obtained by halogen lamps and screens. The incubations began by sealing each core with gastight lids. Benthic incubation time varied from 1 to 3 h to keep O_2 concentration at the end of experiments within 60–70 % of the initial value. The clam stations had shorter incubation times due to their higher O_2 consumption rates. Incubation time was set with pilot incubations carried out before starting the experiments. Nutrients (DIP, NH_4^+, SiO_2) and O_2 concentrations were measured at the beginning and at the end of the incubation. As the NH_4^+ benthic flux is the dominant component of DIN flux (about 90 %) in the SG (Bartoli et al., 2001), NO_3^- and NO_2^- fluxes were not measured. Amperometric O_2 microsensors (Ox-50, UNISENSE A/S, DK) connected to a picoamperometer (Microsensor Multimeter, UNISENSE) were used to measure O_2 concentrations. At time zero, four water samples (60 mL) were collected using plastic syringes from the incubation tanks before cores were capped. At the end of the incubation, lids were removed, and water samples were collected from each core (~750 mL). Samples were filtered through Whatman GF/F glass fiber filters into 20-mL plastic vials, frozen and later analyzed to determine nutrient concentrations (Table 1). Benthic O_2 and nutrient fluxes across the sediment–water interface were calculated according to Eq. (1) (Dalsgaard et al., 2000):

$$F_i = \frac{(C_f - C_o)\cdot V}{A\cdot t} \quad (1)$$

where F_i is the net flux of O_2 or inorganic nutrients measured in dark and light conditions (mmol m^{-2} h^{-1}), C_o is concentration at time zero (mmol L^{-1}), C_f is concentration at the end of incubation (mmol L^{-1}), V is the volume of water in the core (L), A is the area of sediment surface in the core (m^2) and t is the incubation time (h). Daily fluxes (mmol m^{-2} d^{-1}) were then obtained by multiplying hourly fluxes measured in the light (NP, net production) and in the dark (RE, respiration) by the number of light (14 h) and dark hours (10 h) of the sampling period, assuming constant rates. Fluxes directed from the sediment to the water column were considered positive.

Bottom water incubations for each station were performed to determine its contribution to respiration, net primary production, and daily fluxes. The light and dark water incubations were carried out simultaneously in small transparent liners (i.d. 4 cm, length 20 cm, each one with a water volume of ~200 mL, n = 6 for light and n = 6 for dark measurements) maintained in the same tank and lasted 14–16 h. The dark cores from each station were double wrapped in aluminum foil. The stirring system and sampling method were the same as those used in the sediment cores incubation. The volumetric respiration and net production in the dark and light conditions (mmol m^{-3} h^{-1}), respectively, were calculated as the difference between final and initial concentrations. Then, volumetric rates were depth integrated to calculate areal rates (mmol m^{-2} h^{-1}) to allow comparison with benthic fluxes. Daily O_2 fluxes were also measured for *Ulva* sp., and *Gracilaria* sp. The average biomass of algae measured in situ (30 and 110 g_{dw} m^{-2} for *Ulva* sp. and *Gracilaria* sp., respectively) was incubated both in light and dark conditions. The incubation lasted 2–3 h; water samples were collected at the beginning and at the end of the incubation and processed as described for the water column and sediment cores incubations (Table 1).

2.4. Measurements of pore water and sedimentary properties in the SG lagoon

At the end of sediment incubations, pore water was extracted from the upper superficial sediment layer (0–4 cm) using Rhizon™ samplers in large cores. After inserting the samplers, a 10-mL syringe was connected to each one by a luer-lock for water collection. An aliquot was transferred to 5-mL glass vial containing 50 μL of concentrated HNO_3 for dissolved $Fe(II)_{pw}$ and $Mn(II)_{pw}$ analyses via atomic absorption (Varian, Model AA240 Atomic Absorption Spectrometer). Subsamples of 1 mL were transferred to 10-mL glass vials for DIP_{pw} spectrophotometric analysis. Subsamples of 3 mL were transferred to plastic vials and frozen for NH_{4pw}^+ and SiO_{2pw} analyses. For H_2S_{pw}, 1 mL of pore water was immediately transferred into a plastic vial containing 2 mL of 2 % zinc acetate solution to precipitate H_2S_{pw} as ZnS. Free sulphides were determined spectrophotometrically by releasing S^{2-} from the ZnS precipitate using an acidified solution of phenylenediamine and ferric chloride (Cline, 1969).

The remaining sediment in each core was sieved through a 500 μm mesh sieve to determine the clams and other macrofauna species density and biomass. The flesh of the collected clams was then weighed fresh and after drying at 60 °C until constant weight.

Sedimentary features analysis was conducted on subsamples from the upper sediment layer (0–4 cm) in six small cores per station (Table 1). The Chl-a_{sed} was extracted from 1 mL of sediment taken from the upper 1 cm with 5 mL of 90 % acetone and then determined spectrophotometrically (Lorenzen, 1967). Each sediment slice was then homogenized, and sediment subsamples were taken using a cut-off 5 mL syringe. A 1 mL subsample was transferred to a pre-weighted 40 mL glass vial containing 5 mL of 0.5 M HCl to measure solid-phase iron pools. Total iron, hydroxylammine-reducible-ferric iron and HCl-extractable ferrous iron were measured as Fe(II) using the ferrozine method, after extraction from the sediment. Iron reducible with hydroxylammine is considered the more reactive form of ferric iron. The hydroxylammine-reducible-ferric iron plus the 0.5 M HCl extractable-ferrous iron can be considered as total reactive iron, which can be involved in redox processes (Lovley and Phillips, 1987).

Another subsample of sediment (5 mL) was dried at 60 °C until constant weight to measure water content and porosity. Each sample was then homogenized and ground with a porcelain mortar and pestle prior to the analysis of total organic carbon (TOC), total nitrogen (TN) and isotopic composition ($\delta^{13}C$ and $\delta^{15}N$). TOC, TN, $\delta^{13}C$ and $\delta^{15}N$ were measured with a Thermo Fisher Flash HT plus Elemental Analyzer coupled with Delta V Advantage isotope ratio mass spectrometer after the removal of carbonates with HCl (1.0 M), rinsing with deionized water to neutralize the pH and drying the samples at 60 °C. The samples were run in duplicate and the analytical precision of both TOC and $\delta^{13}C$ was ±0.07 %. TOC and TN were corrected for the weight loss during decalcification. For $\delta^{13}C$, the reference was Vienna Pee Dee Belemnite (VPDB), and for $\delta^{15}N$, it was atmospheric nitrogen. Isotopic ratios were expressed in the usual δ-notation (part per mill, ‰). Samples replicate analyses were within ±0.07 % for $\delta^{13}C$ and ±0.14 % for $\delta^{15}N$.

Measurements of $\delta^{13}C$ and $\delta^{15}N$ were also performed for seaweeds biomass (*Ulva* sp., and *Gracilaria* sp.) and clam tissue at St.6 after drying

and powdering in a porcelain mortar. Sample replicates analyses were within ±0.07 % for $\delta^{13}C$ and ±0.35 % for $\delta^{15}N$.

2.5. Calculation of the trophic index, organic matter quality, biogeochemical timescales and anoxic risk in the SG lagoon

2.5.1. The trophic index (TRIX)

The trophic index (TRIX, Vollenweider et al. (1998)) was calculated to characterize the water quality in each station. The TRIX has been used for assessing the risk of eutrophication of different marine ecosystems (Nasrollahzadeh et al., 2008; Cutrim et al., 2019). This index is a linear combination of the logarithms of four variables related to eutrophication: chlorophyll-a, DIN, DIP, and percent deviation from O_2 saturation values. The TRIX was calculated from Eq. (2):

$$TRIX = \frac{\log[\, Chla_{WC} \cdot aD\%O \cdot DIN_{WC} \cdot DIP_{WC}] - [k]}{m} \quad (2)$$

where, Chl-a_{WC} is the concentration of chlorophyll-a in the water column (mg m^{-3}); aD%O (abs|100-%O_2|) is the absolute value of the difference between measured and 100 % dissolved O_2 saturation; DIN_{WC} and DIP_{WC} are the dissolved concentrations of inorganic nitrogen and inorganic phosphorus in the water column, respectively. The constants *k* and *m* are scalar values introduced to adjust the lower limit value of the index and the range of the related trophic scale. Where *k* is the lower limit sum of the required variables for TRIX and *m* is calculated by the difference between the lower and upper limits of each variable, divided by 10 (Nasrollahzadeh et al., 2008). From the monitoring data, the calculated constants values of *k* and *m* were 3.3 and 0.6, respectively.

Trophic scales and descriptors for water quality were adopted from Giovanardi and Vollenweider (2004), Nasrollahzadeh et al. (2008) and Cutrim et al. (2019). Numerically, the index is scaled from 0 to 8, covering a wide range of trophic conditions from ultra-oligotrophic to hypereutrophic (Table 2S, Supplementary material).

2.5.2. Organic matter quality of sediments in the SG lagoon

The contribution of terrestrial and marine organic matter to sediment organic carbon was estimated using a two-end-member mixing model based on the equation derived by Calder and Parker (1968), taken from Schlunz et al. (1999). This approach has been widely applied in marine sediments subjected to organic matter pollution (Zhou et al., 2006; Li et al., 2016; Arroyave Gómez et al., 2020). The terrestrial organic carbon contribution was calculated using Eq. (3):

$$TOC_{Terr}(\%) = \frac{(\delta^{13}C_{marine} - \delta^{13}C_{Org})}{(\delta^{13}C_{marine} - \delta^{13}C_{terrestrial})} \text{ x } 100\% \quad (3)$$

The contribution of marine organic carbon to the TOC was then estimated from Eq. (4):

$$TOC_{Marine}(\%) = 100 - TOC_{Terr}(\%) \quad (4)$$

where $\delta^{13}C_{marine}$ is the $\delta^{13}C$ of marine end member, $\delta^{13}C_{terrestrial}$ is the $\delta^{13}C$ of terrestrial end member and δ^{13}Corg is the measured value in sediment samples. A $\delta^{13}C_{terrestrial}$ value of - 27.23 ‰ was used as end member based on the low $\delta^{13}C$ values of sediment samples in the study area (Magri et al., 2020). For the marine end member ($\delta^{13}C_{marine}$) a value of −22.0 ‰ was used as this isotopic composition considers the contribution of seaweed and clam (*Ruditapes philippinarum*) tissue in the SG Lagoon for the summer season (Bianchini et al., 2021). We also corroborated this value through $\delta^{13}C$ measurements for seaweeds (*Ulva* sp. and *Gracilaria* sp.) and clam tissue at St.6.

2.5.3. Benthic nutrient turnover

The nutrient turnover time is the time (days) required to replenish water column nutrient pools via nutrient recycling from sediments, and under steady state conditions. This parameter provides an estimate of the importance of sediment-water interface exchange processes as nutrient sources to the overlying water column. Turnover time is obtained by the ratio between the water column nutrient pool and the daily benthic flux (Pratihary et al., 2009).

Table 2
Results of Kruskal-Wallis (KW) to test significant difference between stations for parameters of water column, sedimentary features, pore water, and daily O_2 and nutrient fluxes of pelagic and benthic compartment in the SG during summer 2023.

Dependent variable	χ^2	p-value	Pairwise Dunne test
Water quality			
Temperature	33.97	**<0.0001**	St.3-St.5, St.3-St.6, St.4-St.5, St.4-St.6
Salinity	31.31	**<0.0001**	St.1-St.6, St.2-St.4, St.2-St.6, St.5-St.6
DO_{WC}	33.44	**<0.0001**	St.1-St.3, St.1-St.6, St.2-St.3, St.3-St.4
DIP_{WC}	28.75	**<0.0001**	St.1-St.3, St.1-St.4, St.1-St.6, St.2-St.6
NH_{4WC}^{+}	33.02	**<0.0001**	St.1-St.4, St.1-St.6, St.2-St.4, St.2-St.6
NO_{3WC}^{-}	24.33	**<0.002**	St.1-St.4, St.3-St.5, St.4-St.5
DIN_{WC}	29.45	**<0.0001**	St.1-St.4, St.1-St.6, St.2-St.4, St.4-St.5
SiO_{2WC}	24.55	**<0.002**	St.1-St.3, St.2-St.3, St.2-St.6, St.3-St.5
Chl-a_{WC}	27.66	**<0.0001**	St.2-St.6, St.3-St.5, St.3-St.6
TRIX	29.55	**<0.0001**	St.1-St.4, St.1-St.6, St.2-St.4, St.2-St.6
Sedimentary features			
TOC	32.06	**<0.0001**	St.1-St.4, St1.-St.6, St.3-St.4, St.3-St.6
TN	33.278	**<0.0001**	St.2-St.3, St.3-St.4, St.3-St.6
$\delta^{13}C$	25.74	**<0.0001**	St.1-St.3, St.1-St.4, St.1-St.6, St.2-St.6
$\delta^{15}N$	33.356	**<0.0001**	St.2-St.3, St.2-St.5, St.3-St.4, St.3-St.6, St.4-St.5, St.5-St.6
TOC_{Terr}	31.144	**<0.0001**	St.1-St.3, St.1-St.4, St.1-St.6, St.2-St.6
Chl-a_{Sed}	21.72	**<0.0001**	St.2-St.3, St.3-St.4, St.3-St.5
Fe_{tot}	23.45	**<0.0001**	St.1-St.4, St1.-St.6
$Fe(III)_{Sed}$	11.22	**<0.05**	St.3-St.6
Pore water			
DIP_{pw}	30.29	**<0.0001**	St.1-St.4, St.1-St.5, St.1-St.6, St.3-St.6
NH_{4pw}^{+}	22.99	**<0.0001**	St.2-St.3, St.3-St.4, St.3-St.6, St.4-St.5
H_2S_{pw}	16.61	**<0.005**	St.1-St.3, St.2-St.3, St.3-St.4, St.3-St.5
SiO_{2pw}	13.16	**<0.05**	–
$Mn(II)_{pw}$	20.86	**<0.001**	St.2-St.5, St.4-St.5, St.5-St.6
$Fe(II)_{pw}$	24.21	**<0.0002**	St.1-St.3, St.2-St.3, St.3-St.5
SO_{4pw}^{2-}	24.90	**<0.0002**	St.1-St.4, St.1-St.6, St.2-St.6
$Fe(II)_{pw}$: DIP_{pw}	29.28	**<0.0001**	St.1-St.6, St.3-St.5, St.3-St.6
Daily benthic fluxes			
O_{2Bc}	29.22	**<0.0001**	St.1-St.2, St.1-St.4, St.3-St.4, St.4-St.5
DIP_{Bc}	23.92	**<0.0001**	St.1-St.4, St.3-St.4, St.4-St.6
NH_{4Bc}^{+}	15.58	**<0.01**	St.1-St.4, St.4-St.5, St.4-St.6
SiO_{2Bc}	9.12	0.1044	
Daily pelagic fluxes			
O_{2Pg}	31.54	**<0.0001**	St.1-St.3, St.2-St.3, St.3-St.4, St.3-St.5, St.3-St.6, St.4 -St.5
DIP_{Pg}	25.56	**<0.001**	St.1-St.6, St.2-St.5, St.2-St.6
NH_{4Pg}^{+}	27.43	**<0.0001**	St.1-St.3, St.1-St.4, St.1-St.6, St.2-St.3, St.2-St.4
SiO_{2Pg}	21.80	**<0.001**	St.1-St.3
Anoxia risk			
$NetO_2D$	31.354	**<0.001**	St.1-St.3, St.1-St.4, St.3-St.5, St.4-St.5
T_{Anoxia}	29.017	**<0.001**	St.1-St.2, St.1-St.4, St.2-St.5, St.4-St.5

2.5.4. Timescale to the onset of anoxia (T_{Anoxia})

The degree of O_2 depletion depends on the magnitude of the net O_2 sink and the duration for which this O_2 sink occurs. Specifically, hypoxia and ultimately anoxia will occur when sinks exceed sources for long enough to drive O_2 below the hypoxic/anoxic thresholds from its initial concentration (Fennel and Testa, 2019). The timescale to anoxia occurrence or the onset of anoxia (T_{Anoxia}), formally defined by Fennel and Testa (2019), indicates how long it will take for a control water volume to reach anoxia conditions from an assumed initial O_2 concentration. This timescale was calculated for each station using Eq. (5):

$$T_{Anoxia} = \frac{O_{2in}}{NetO_2D} \quad (5)$$

where O_{2in} (mmol O_2 m^{-2}) is the initial O_2 availability at each station and was calculated from DO_{WC} and depth of the water column. The daily O_2 net consumption rate ($NetO_2D$ [mmol O_2 m^{-2} d^{-1}]) was considered a

positive value in Eq. (5) and was calculated from Eq. (6):

$$NetO_2D = \left(O_{2Bc} + O_{2Pg} + O_{2Alg}\right) + R_{Air} \quad (6)$$

where O_{2Bc} is the daily O_2 flux measured in benthic compartment in incubations of intact sediment cores (mmol O_2 m^{-2} d^{-1}), O_{2Pg} is the daily O_2 flux measured in pelagic compartment in water incubations (mmol O_2 m^{-2} d^{-1}) and O_{2Alg} is the daily O_2 flux measured for seaweeds (*Ulva* sp. and *Gracilaria* sp.) in water incubations (mmol O_2 m^{-2} d^{-1}), respectively. Negative daily O_2 fluxes (e.g. O_{2Bc}, O_{2Pg} and O_{2Alg}) indicate oxygen consumption plus physical supply by the air-water exchange in Eq. (6). R_{Air} is the reaeration coefficient (mmol O_2 m^{-2} d^{-1}) and was estimated for each station using Eq. (7):

$$R_{Air} = k_1 (C_{Sat} - C_{WC}) \quad (7)$$

where k_1 is the O_2 exchange coefficient between the water surface and the atmosphere (m h^{-1}), C_{WC} is the DO concentration in the water column and C_{Sat} is the O_2 concentration at saturation (mmol O_2 L^{-1}). A positive value of R_{Air} represents input of O_2 from the atmosphere to the water. The calculation of C_{Sat} and k_1 were performed with equations outlined by Staehr et al. (2010). C_{Sat} was derived from the equation of Weiss (1970) and corrected for barometric pressure. k_1 was calculated using Eqs. 8–10:

$$k_1 = k_{600}\left(\frac{Sc}{600}\right)^{-1/2} \quad (8)$$

The Schmidt number (Sc) is required to determine the physical air-water O_2 exchange. Sc is calculated as a function of water column temperature (Wanninkhof, 1992):

$$Sc = 0.0476T^2 + 3.7818T^2 - 120.1T + 1800.6 \quad (9)$$

k_{600} is estimated as a function of wind speed at 10 m above the surface of SG Lagoon. The average wind speed was obtained from hourly value in each station by the hydrodynamic model SHYFEM (Umgiesser et al., 2004):

$$k_{600} = \frac{\left(2.07 + 0.215U_{10}^{1.7}\right)}{100} \quad (10)$$

The T_{Anoxia} was assessed for three different scenarios of Re-aeration coefficient (Eq. (7)) to analyze its effect on this timescale. (i) C_{WC} = 30 % saturation O_2, (ii) C_{WC} = 100 % saturation O_2 and (iii) C_{WC} = daily average concentration (O_2mean) is equal to that obtained in the sampling of the water column in each station.

2.5.5. Statistical analyses of experimental data

Kruskal-Wallis (KW) test was applied to verify significant ($p < 0.05$) univariate differences between stations for water quality, sedimentary properties, pore water and daily nutrient fluxes because data did not fulfill the assumption of normality. When KW was significant, the Dunn's post-hoc test was used to obtain pairwise comparison results. The p-values were adjusted with the Bonferroni method.

Correlations between biogeochemical drivers and response variables were analyzed using simple and multiple linear regression models, Pearson's correlations (significance level $p < 0.05$) and redundancy analysis (RDA), respectively.

RDA was used to assess the influence of a broader range of potential drivers (e.g., pore water, sedimentary features, water quality, and clams' density) on nutrient daily fluxes and biogeochemical timescales (response variables). Before RDA analysis, (i) a Detrended Correspondence Analysis (DCA) was used to determine the length of the gradient. Results showed that the gradient length represented by the first ordination axis was shorter than 3 SD (standard deviation). This corresponded to a linear data structure; therefore, the RDA can be used to determine the functional relationship between explanatory and response variables. (ii) A data exploratory multivariate analysis through Principal Component Analysis (PCA) was made on biogeochemical drivers (explanatory variables) to detect and remove redundant variables leading to multicollinearity and affecting data interpretation (data not shown). The variance inflation factor (VIF <2) was also monitored, as an indicator, to reduce the collinearity among explanatory variables (Zuur et al., 2010).

After removing redundant variables, RDA models with the set of environmental variables that best explained the nutrient daily fluxes and biogeochemical timescales were selected through a forward stepwise process (''ordistep'' function in R-package 'vegan', model choice comparing AIC scores). The statistical significance of the RDAs was tested against 999 permutations of ANOVA, with a p-value <0.05. RDA results were interpreted based on the scaling 2. Angles between all vectors reflect linear correlation (Legendre and Legendre, 1998).

All analyses and graphs were performed using the R computational framework version 4.3.0 (R Core, 2020). The R-package 'corrplot' was used to perform Pearson's analysis (Wei et al., 2017). RDA was made using the R-package 'vegan' (Oksanen et al., 2013). Graphs were made with R-package 'ggplot2'(Wickham et al., 2016).

2.5.6. Horizontal and vertical transport timescales in the SG lagoon during summer 2023

The horizontal timescales in each station were estimated by the hydrodynamic model SHYFEM (System of HydrodYnamic Finite Element Modules; Umgiesser et al., 2014), an open-source 3D hydrodynamic model that operates on unstructured triangular meshes (https://github.com/georgu/shyfemcm-ismar). The model with its finite element approach provides a key advantage for complex bathymetric environments, such as shallow coastal waters and continental shelf seas, by allowing variable grid resolution to enhance accuracy in regions requiring finer detail (Umgiesser et al., 2004). The model has previously been applied to the SG Lagoon and has been calibrated and validated (Valentini et al., 2019; Maicu et al., 2021).

The setup of the model used in this study differs from the previous implementations mainly due to the modeled domain, which is larger than in the previous studies, including parts of the Adriatic shelf. The numerical domain consists of 45,400 nodes and 81,879 elements, with a maximum depth of approximately 55 m offshore, structured into 27 vertical z-levels, where the first layer has a thickness of 1.5 m. The horizontal mesh size varies from 10 m in the Po branches to 3 km in the open sea. More details are given in Biolchi et al. (2025).

The simulation was configured for the year 2023, using observed Po River discharge and temperature data at the Pontelagoscuro station. Open boundary conditions in the Adriatic Sea were obtained from the Copernicus Marine Environment Monitoring Service (CMEMS; https://doi.org/10.25423/CMCC/MEDSEA_ANALYSISFORECAST_PHY_006_013_EAS8) (Clementi et al., 2021), providing hourly vertical outputs of salinity, temperature, and current velocities, as well as total sea level, including the astronomical tide component. Atmospheric forcing at the surface was supplied by a high-resolution (2.2 km) implementation of the COSMO meteorological model (Steppeler et al., 2003) for the Italian territory (Gastaldo et al., 2021). The meteorological inputs include 10-m zonal and meridional wind components, 2-m air temperature and dew point temperature, mean sea level pressure, precipitation, total cloud cover, and net shortwave radiation flux. Other details on how the model was set up can be found in Biolchi et al. (2025).

The horizontal transport timescale was estimated by computing an e-folding flushing time (T_f). The lagoon was filled with a conservative tracer and its decay was computed. By either integrating the curve or by fitting the log of the concentration to a line, the T_f was estimated for each point in the lagoon. Both approaches gave approximately the same values. This procedure was repeated every 14 days to produce flushing time data every two weeks. Details can be found in Cucco and Umgiesser (2006) and Umgiesser et al. (2016). The e-folding flushing time is a timescale commonly used to measure the water retention time in aquatic ecosystems (Monsen et al., 2002), and integrates the net effect of all

flushing processes acting on the SG such as the tidal exchange flow from Adriatic Sea and river inputs (Cucco and Umgiesser, 2006). Additionally, in this work it was decided to follow the e-folding flushing time approach, to be consistent and to compare the results with those reported by Maicu et al. (2021). The vertical mixing timescale (T_V) was estimated through the vertical turbulent diffusion coefficient (K_V), obtained from the model and depth (H) in each station using Eq. (11) (Lucas and Deleersnijder, 2020):

$$T_V = \frac{H^2}{K_V} \tag{11}$$

2.5.7. Spatial analysis of anoxia risk in SG lagoon

The nondimensional number (γ), defined by Fennel and Testa (2019), relates the timescale of anoxia occurrence (T_{Anoxia}) to the water residence time (T_R) by Eq. (12):

$$\gamma = \frac{T_{Anoxia}}{T_R} \tag{12}$$

when $\gamma < 1$ (biogeochemical O_2 depletion is faster than replenishment) occurs an anoxia event. However, in Eq. (12), the water residence time does not account for the vertical exchange that is a key parameter for DO replenishment in estuaries characterized by long water residence time. Recently, Shen and Qin (2024) demonstrated that the shortest timescale between vertical and horizontal transport is the dominant factor physically controlling the DO replenishment in estuaries. Shen and Qin (2024) introduced that if the vertical transport timescale is much shorter than the horizontal transport timescale ($T_V \ll T_R$), γ should be calculated by Eq. (13) for the anoxia condition. In contrast, if the horizontal transport is much shorter than the vertical transport ($T \ll T_V$), γ should be estimated by Eq. (12).

$$\gamma_V = \frac{T_{Anoxia}}{T_V} \tag{13}$$

Maps were made from data collected at the six sampling stations for T_{Anoxia} and γ using the Inverse Distance Weighting (IDW) interpolation technique in the ArcGIS 10.8 software. In the IDW, the interpolation is estimated based on the values at neighboring locations, primarily weighted by distance from the interpolation location. The IDW is one of the commonly used techniques for spatial interpolation methods in GIS (Lu and Wong, 2008). Additionally, maps for nutrient benthic turnover were also created to assess the spatial variation of the nutrient replenishment in the SG Lagoon.

3. Results

3.1. Spatial variability of water quality parameters and TRIX for the SG lagoon

Features of water quality and trophic state for the SG are summarized in Fig. 2. Stations influenced by riverine and freshwater channels (St.1, St.2 and St.5) had higher nutrient and lower DO_{WC} average concentrations than stations influenced by marine water (St.3, St.4 and St.6). The water quality in the northwestern area (St.1, St.2) of the lagoon was lower than in the central and southeastern zone (St.4, St.5 and St.6) during the sampling (Figs. 1 and 2). This pattern is confirmed by the KW test and pairwise comparison between stations for all the measured parameters (Table 2 and Fig. 2). According to the relationship between the trophic level and water quality descriptors (Table 2S), the SG waters ranged from very productive and high trophic status (TRIX 6–8) at St.1 and St.2 to poorly productive and low trophic status (TRIX 2–4) at marine stations (St.4 and St.6) (Fig. 2J).

3.2. Spatial variability of sedimentary features, organic matter quality and pore water chemistry at the SG lagoon

Sediments from the three stations with clams were sandy and were markedly different in terms of density, porosity, water content, TOC, TN and $\delta^{15}N$ signatures compared to the stations without clams (Table 3S and Fig. 3). The average TOC ranged from 0.15 ± 0.02 % at St.6 to 0.36 ± 0.05 % at St.2 in clams farmed stations, while outside farmed areas, TOC varied from 1.34 ± 0.03 % at St. 5 to 1.77 ± 0.13 % at St.3 (Fig. 3A). Higher average TOC values were observed at non-farmed stations (St.1 and St.3), that were significantly different from clams farmed stations (St.4 and St.6) (Table 2). The mean TN was lower than the detection limit at clam stations, whereas at stations without clams, values ranged from 0.22 ± 0.01 % at St. 1 to 0.31 ± 0.03 % at St.3 (Fig. 3B). Pairwise comparisons suggested significant differences between TN values measured at St.3 and those measured at clam sites, but not between St.1 and St.5 (Table 2). The northwestern stations (St.1 and St.2) displayed more depleted $\delta^{13}C$ signatures as compared to stations located in the central and southeastern area (Fig. 3C). The average relative contribution of TOC_{terr} ranged from 94.28 ± 1.18 % at St.1 to 21.21 ± 3.19 % at St.6 according to two-end-member mixing model. Although St.1 and St.3 had similar average TOC (Fig. 3A), their $\delta^{13}C$ signatures and therefore TOC_{Terr} were significantly different (Fig. 3 and Table 2). The lower contribution of TOC_{terr} at St.3 was consistent with the high Chl-a concentrations found in the water column and in the superficial sediment at this site during sampling (Figs. 2I and 3G). The average $\delta^{15}N$ signatures were quantified only at sites without clams. The most depleted average $\delta^{15}N$ values were found at St.1, whereas the signatures were similar at St.3 and St.5 (Fig. 3D). Pairwise comparisons of $\delta^{15}N$ indicated significant differences between clams farmed stations and St.3 and St.5, but not with St.1 (KW and Dunnet's test, $p < 0.05$, Table 2). The molar ratio TOC:TN showed little variation, ranging between 6 and 7 at sites without clams. The average Fe(III) oxyhydroxide ranged from 2.02 ± 0.90 % at St.3 to 13.08 ± 3.64 % at St.6 (Fig. 3H and I). Pairwise comparison showed a significant difference between these two stations (Table 2).

The DIP_{pw}, NH_{pw}^{+} and $Mn(II)_{pw}$ were generally higher at stations without clams (Fig. 4 and Table 2). Sediments at St.3 were chemically reduced with high average TOC (~50 % terrestrial OC, Fig. 3F), H_2S_{pw} and NH_{pw}^{+} concentrations. The variation in SO_{pw}^{2-} concentration overlapped that of salinity (Figs. 2B and 4G), with lower values at St.1, and higher values at St.6. The highest average $Fe(II)_{pw}$:DIP_{pw} molar ratio was found at St.6 (0.16 ± 0.08), while the lowest was calculated at St.3 (~0). These values correspond to the highest and lowest average Fe(III) oxyhydroxide concentrations measured at St.6 and St.3, respectively (Figs. 3I and 4H).

3.3. Oxygen and nutrients daily budget in the benthic and pelagic compartments of the SG lagoon

The daily O_{2BC} fluxes in the SG were negative at all stations (Fig. 5A). The highest average daily O_{2BC} consumption was found at St.4 (−468.09 ± 60.47 mmol O_2 m^{-2} d^{-1}), where the greatest average clam biomass was recorded (481.05 ± 91.54 g $_{DW}$ m^{-2}). In contrast, the lowest O_{2BC} consumption was measured at St.1, which had no clams (−54.11 ± 5.62 mmol O_2 m^{-2} d^{-1}) (Figs. 5A and 6D). Overall, stations with clams displayed higher daily O_{2BC} consumption compared to those without clams. Although, the St.6 did not show significant differences from any station without clams (KW and Dunnet's test, $p < 0.05$, Table 2). Daily O_{2BC} fluxes and clam biomass were negatively correlated (Fig. 6A). The intercept of the regression line calculated using 36 sediment cores was −56.8 mmol O_2 m^{-2} d^{-1} and represents the theoretical average O_2 demand of the SG sediments, excluding the contribution of clams to respiration. The daily O_{2BC} consumption at clam sites was around 4.5 times higher than the respiration measured in the 18 cores without clams. On the other hand, the depth integrated daily O_{2pg} flux in the

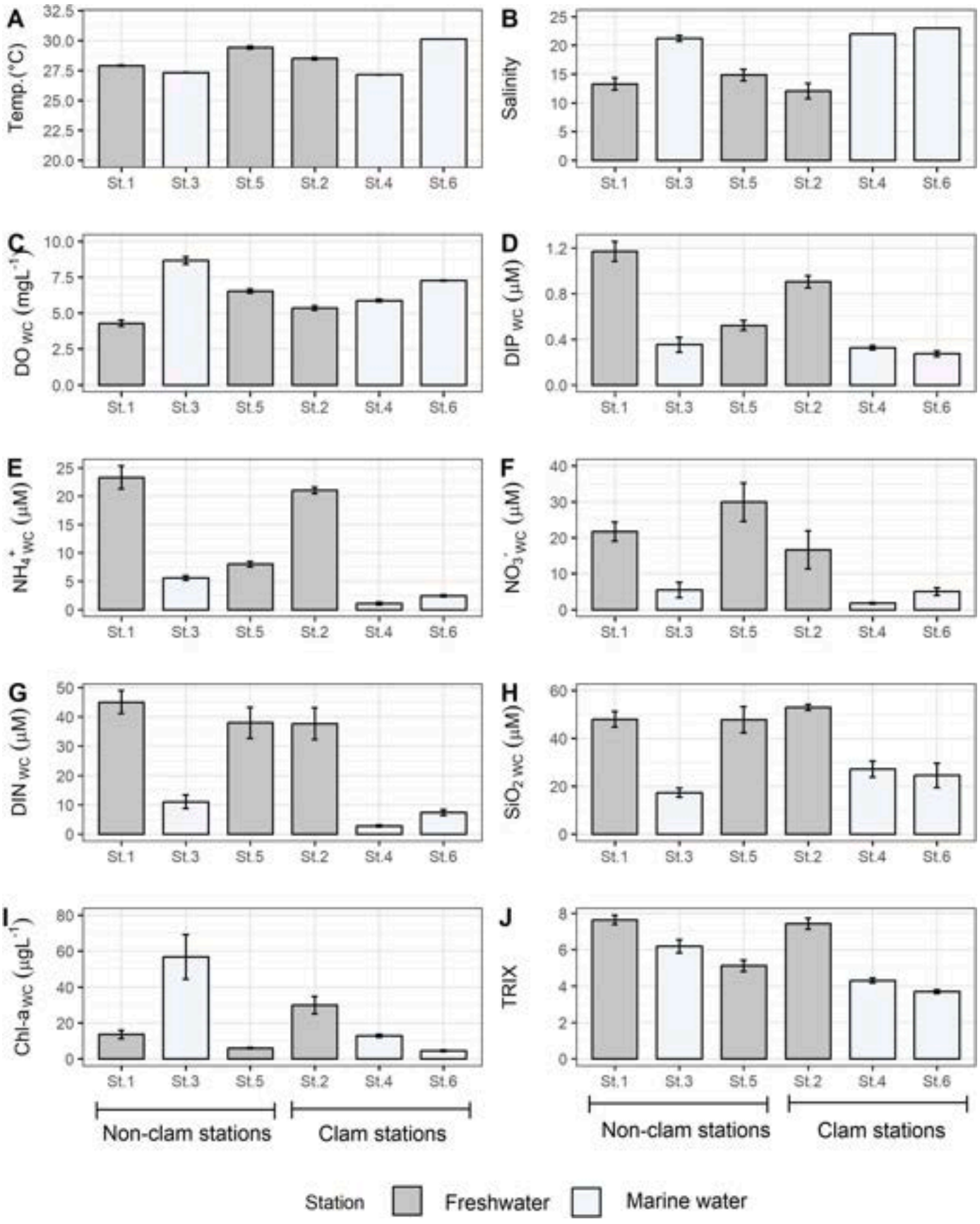

Fig. 2. Summary of water quality parameters and trophic status classification in six stations of the SG Lagoon sampled during summer 2023. **(A)** Water temperature, **(B)** Salinity, **(C)** DO_{wc}, **(D)** DIP_{WC}, **(E)** NH_{4WC}^{+}, **(F)** NO_{3WC}^{-}, **(G)** DIN_{WC}, **(H)** SiO_{2WC}, **(I)** Chl-a_{WC} and **(J)** Trophic index (TRIX). (Stations without clams: St.1, St.3 and St.5; Stations with clams St.2, St.4 and St.6). (Average ± standard error, n = 6).

Table 3
Relative contribution of benthic and pelagic processes and of macroalgae to total daily O_2 consumption in SG Lagoon during summer 2023.

Station	Sediment (%)	Water column (%)	Macroalgae (%)
St.1	63.13 ± 3.32	36.87 ± 3.32	0 %
St.2	85.12 ± 2.20	14.88 ± 2.20	0 %
St.3	13.81 ± 5.94	86.19 ± 5.94	0 %
St.4	91.50 ± 1.02	8.50 ± 1.02	0 %
St.5	~100.00	0 %	0 %
St.6	61.50 ± 3.18	17.31 ± 1.38	21.19 ± 2.24[a]

[a] The daily O_2 consumption of *Ulva* sp. and *Gracilaria* sp. was 20.11 ± 0.72 % and 79.89 ± 0.66 % of total macroalgae consumption, respectively.

pelagic compartment was negative at all stations except for St.5, where its value was around zero. The highest depth integrated daily O_{2pg} was measured at St.3, the deepest station with the highest Chl-a concentration (Fig. 5B and Table 2).

Some general patterns emerged for the NH_4^+ and DIP fluxes in both the benthic and pelagic systems. Daily, sediment was a source of NH_{4BC}^+ and DIP_{BC} at all the stations. The highest average daily NH_{4BC}^+ and DIP_{BC} fluxes were found at St. 4 with 34.19 ± 5.27 mmol NH_4^+ m^{-2} d^{-1} and 3.61 ± 0.78 mmol DIP m^{-2} d^{-1}, respectively (Fig. 5C and E). The daily NH_{4BC}^+ and DIP_{BC} fluxes at St.4 showed significant differences compared to the other stations (KW and Dunnet's test, $p < 0.05$, Table 2). Both benthic fluxes were positively correlated with the clam biomass. The daily NH_{4BC}^+ and DIP_{BC} fluxes from sediments, excluding contribution of clams, were 2.97 mmol NH_4^+ m^{-2} d^{-1} and 0.47 mmol DIP m^{-2} d^{-1}, respectively. Such values are the intercepts of the linear regressions between NH_4^+ and DIP fluxes and clam biomass (Fig. 6B and C). On average, the daily NH_{4BC}^+ and DIP_{BC} fluxes were around 5.8 and 3.8 times higher at clams farmed than at non farmed sites, respectively. The depth integrated daily NH_{4Pg}^+ and DIP_{Pg} in the pelagic system were negative at St.1 and St.2, which is consistent with the eutrophic status and greater concentration of these nutrients in the water column (Fig. 2). The pairwise comparison of these stations with the others for NH_{4Pg}^+ and DIP_{Pg} is shown in Table 2.

The daily SiO_{2BC} fluxes did not display a clear difference, as observed for O_{2BC}, NH_{4BC}^+ and DIP_{BC}, between sites with and without clams, and SiO_{2BC} fluxes were not correlated with clam biomass (Table 2). While the St.2 and St.6 acted as a sink of SiO_{2BC}, the St.4 was a weak source. Depth integrated daily SiO_{2Pg} showed significant differences between St.1-St.3.

3.4. Timescales of anoxia onset and nutrient turnovers in stations with and without clams in the SG lagoon

The contribution of daily O_{2BC} to $NetO_2D$ was higher than that of O_{2Pg} in all stations except for St.3 (Fig. 7A and Table 4). Daily O_{2BC} at clam stations 2 and 4 was responsible for up to 80–90 % of total O_2 consumption, whereas this share was lower at the St.6 (~60 %), with *Ulva* sp. and *Gracilaria* sp. respiration accounting for ~20 % of $NetO_2D$ (Fig. 7A and Table 3). The reaeration coefficient reported in Fig. 7A was estimated from the average O_2 concentration obtained in the water column during the sampling (O_2 mean). We calculated an O_2 vertical replenishment by reaeration at St.1, St.2, St.4 and St.5, and an outgassing across the air–sea interface at St.3 and St.6. Pairwise comparison suggests significant differences in $NetO_2D$ values between both the deepest site (St.3) and the highest clam biomass site (St.4) and the stations St.1 and St.5 (Table 2).

The effect of the reaeration coefficient on the T_{Anoxia} was assessed in three different scenarios (C_{WC} = 30 % saturation O_2, C_{WC} = 100 % saturation O_2 and C_{WC} = O_2mean) (Fig. 7B). The influence of reaeration was higher at shallow stations without clams (St.1 and St.5) compared to stations with clams and the deepest station (St.3). From results of reaeration coefficient, we calculated the T_{Anoxia} from O_2mean as we considered O_2mean as a realistic condition between 30 % and 100 % of O_2 saturation.

The calculated anoxia timescale and nutrient turnover times (NH_4^+ and DIP) at all stations are shown in Fig. 7C. The SiO_2 turnover time was not calculated because ~70 % of the daily fluxes were negative. Overall, clam stations showed shorter T_{Anoxia} (faster O_2 consumption rates) and shorter nutrient benthic turnovers (faster nutrient recycling) than the sites without clams. The St.4 had the shortest T_{Anoxia}, T_{NH4} and T_{DIP} than the other stations, with average values of 0.19 ± 0.02 d, 0.02 ± 0.004 d and 0.05 ± 0.01 d, respectively. These outcomes mean that a clam biomass of 481.05 ± 91.54 g_{dry} m^{-2} can produce a significant drop in O_2 concentration in the water column in ~4.5 h and that the benthic fluxes can replenish the whole pelagic NH_4^+ and DIP inventory in ~0.5 h and 1.2 h, respectively, under steady state condition. Pairwise comparison suggests significant differences for T_{Anoxia} between stations with high clam biomass (St.2 and St.4) and the non-farmed sites St.1 and St.5 (KW and Dunnet's test, $p < 0.05$, Table 2).

3.5. Biogeochemical drivers of the timescale of anoxia onset

A correlation analysis was made on the benthic system by Pearson's correlation after removing redundant variables of the pelagic compartment by PCA (Fig. 8). The TOC and TN had a high collinearity ($r = 0.98$, $p < 0.0001$, Fig. 8). Since the TOC was measured at all the stations, the TN was removed, and TOC was retained for subsequent analyses. The Pearson's correlations between biogeochemical drivers (sedimentary features and pore water) and timescales (T_{Anoxia}, T_{HN4} and T_{DIP}) in the benthic compartment showed that TOC was highly correlated with all of these parameters, except with $Fe(II)_{pw}$ (Fig. 8). A negative correlation was found between TOC and clam biomass ($r = -0.73$, $p < 0.0001$, Fig. 1S). Biogeochemical timescales had a significant positive correlation with TOC, $\delta^{15}N$, DIP_{pw} and NH_{4pw}^+, whereas they showed a strong negative correlation with clam biomass, $Fe(II)_{pw}$:DIP_{pw} ratio and SO_{4pw}^{2-}. On the other hand, T_{Anoxia} and T_{NH4} were negatively correlated with $\delta^{13}C$ and positively correlated with $Mn(II)_{pw}$. Instead, T_{Anoxia} and T_{DIP} had negative correlation with the percentage of Fe(III) calculated over the total Fe pool.

The RDA analysis showed that the clam biomass was the main driver of daily benthic fluxes, explaining approximately 40 % of variation on the axis RDA1 (Fig. 9A and Table S4 in the Supplementary material). Results from the RDA for daily benthic fluxes (Fig. 9A) align with those found through Pearson pairwise correlations (Fig. 8). Additionally, since SiO_{2Bc} was not correlated with clam biomass, an RDA model excluding this benthic flux was carried out and showed an increase of the explained portion of the clam biomass on the total variation by about 53 % on the response variables (O_{2Bc}, NH_{4Bc}^+ and DIP_{Bc}) (not shown). On the other hand, the clam biomass and NH_{4pw}^+ were the most significant variables explaining 29 % of changes in the biogeochemical timescales in the two axes that were statistically significant (Fig. 9B and Table 5S Supplementary material). The NH_{4pw}^+ was chosen over the TOC to represent the organic matter in the model because there was a high collinearity between clam biomass and TOC according to VIF (>2). The clam biomass had a higher negative correlation with T_{Anoxia} and T_{NH4} than with T_{DIP}, whereas NH_{4pw}^+ showed a greater positive correlation with T_{NH4} and T_{DIP} than with T_{Anoxia}. Regarding biogeochemical timescales, T_{Anoxia} had a stronger positive correlation with T_{NH4} than with T_{DIP}.

3.6. Spatial variability of timescales of anoxia onset and nutrient turnover

The timescale of anoxia onset was shorter in the clam farming area and in the deepest zone around St.3 than at sites without clams towards the northwestern (St.1) and southeastern (St.5) part of the lagoon. While the drop in water column O_2 concentration to anoxia level can take around 0.19–0.76 d in clams farming areas and around St.3, in the rest of the lagoon this can take about 1.2–1.9 d (Fig. 10 A). However, the smaller timescale of anoxia in the area near the St.3 was due to high contribution in the depth integrated daily O_{2pg} of the pelagic

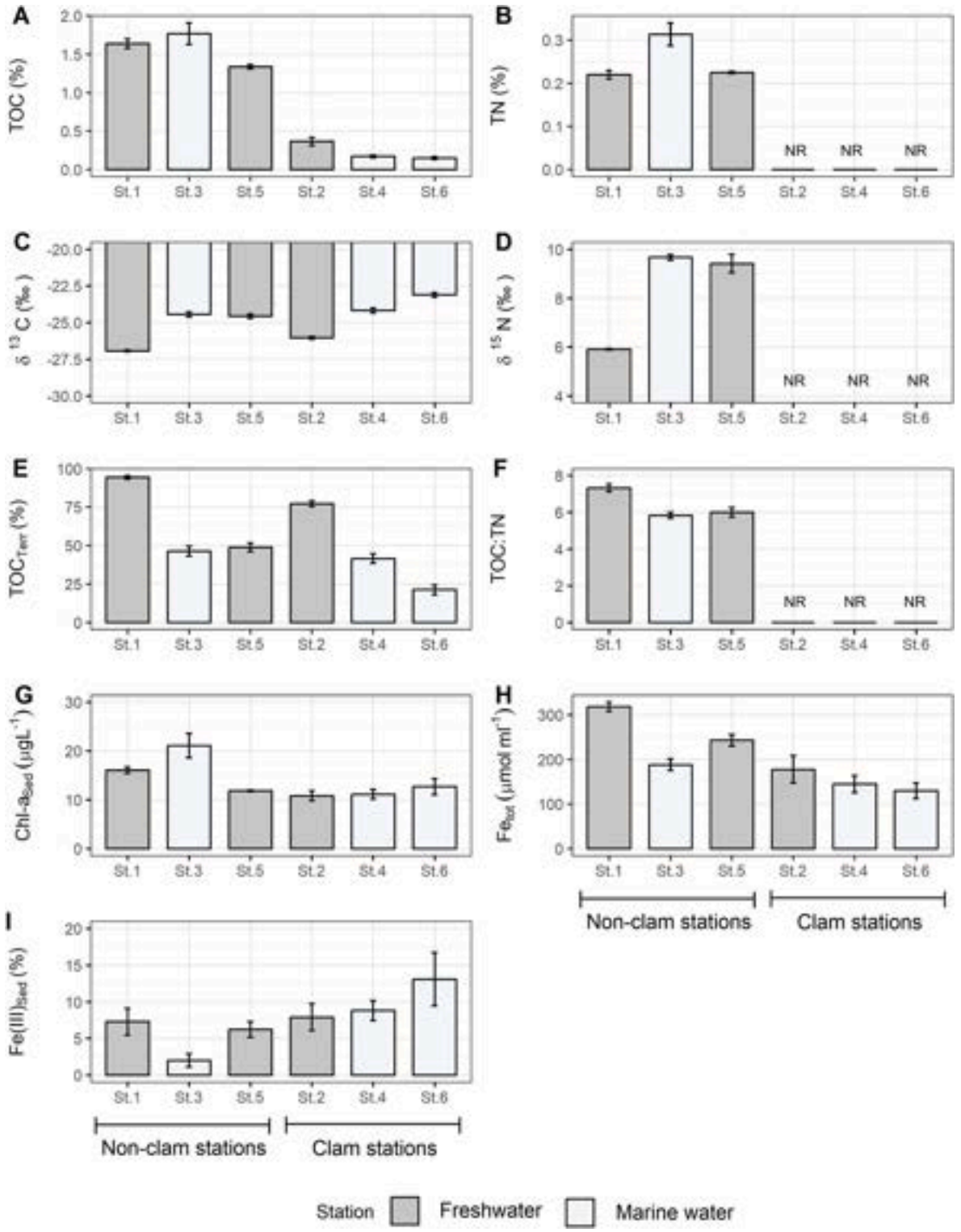

Fig. 3. Summary of sedimentary features measured in the upper layer (0–4 cm) in six stations of the SG Lagoon sampled during summer 2023. **(A)** TOC, **(B)** TN, **(C)** $\delta^{13}C$, **(D)** $\delta^{15}N$, **(E)** TOC_{Terr}, **(F)** TOC:TN molar ratio, **(G)** Chl-a_{sed}, **(H)** Fe_{tot} and **(I)** $Fe(III)_{sed}$ (Stations without clams: St.1, St.3 and St.5; Stations with clams St.2, St. 4 and St.6). (Average ± standard error, n = 6). Note: TN and $\delta^{15}N$ values are not reported (NR) as concentrations were close to the detection limit of the method.

compartment rather than benthic respiration (Fig. 5b). Therefore, the timescale of anoxia onset is approximately 2–10 times faster (smaller timescales) in the clam farming areas as compared to surrounding non-farmed shallow stations.

Overall, the spatial pattern of T_{NH4} was similar to T_{Anoxia} (Fig. 10 B). The T_{NH4} varied from 0.02 to 1.05 d in clam farming areas, while it ranged from 2.09 to 3.11 d in non-farming sites. This indicates that the replenishment rate of NH_4^+ from the benthic to the pelagic system in clam farming area can be from 3 to 100 times faster, under steady state conditions, as compared to non-farmed sites. On the other hand, the spatial variability of T_{DIP} was different from that of T_{Anoxia} and T_{NH4}. The T_{DIP} varied by one order of magnitude and ranged from 0.05 to 0.61 d in

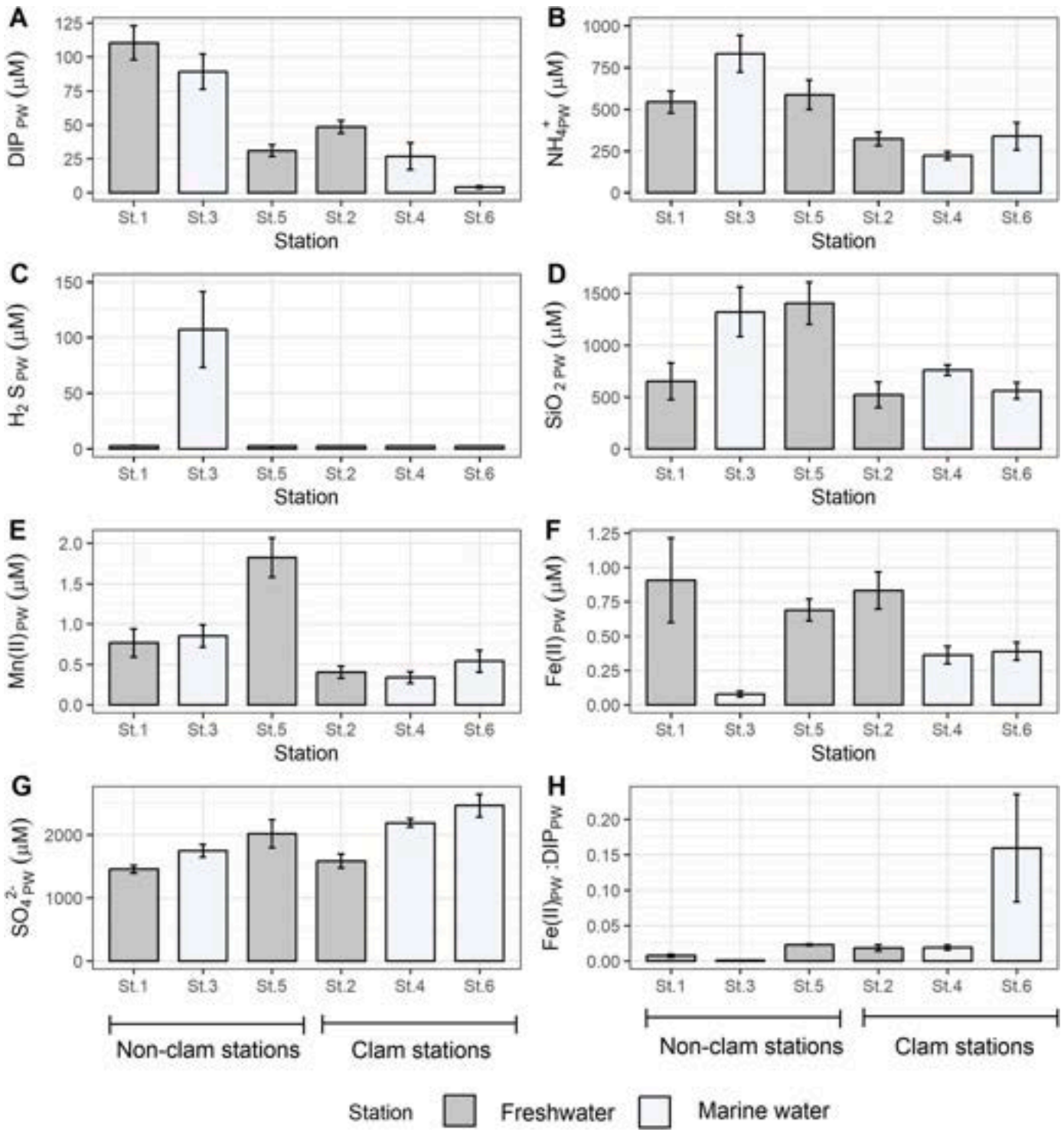

Fig. 4. Summary of surface pore water parameters (0–4 cm) in six stations of the SG Lagoon measured during summer 2023. **(A)** DIP_{pw}, **(B)** NH_{pw}^{+}, **(C)** H_2S_{pw}, **(D)** SiO_{2pw}, **(E)** $Mn(II)_{pw}$, **(F)** $Fe(II)_{pw}$, **(G)** SO_{pw}^{2-} and **(H)** $Fe(II)_{pw}$:DIP_{pw} (Stations without clams: St.1, St.3 and St.5; Stations with clams St.2, St. 4 and St.6). (Average ± standard error, n = 6).

the clam farms and in the southeastern area (around St.5) of the SG while it varied from 0.77 to 1.32 d in the northern area. However, the DIP turnover (0.05–0.19 d) at St.4 was ~5–26 times faster than at St.3 and St.5 (1.05–1.32 d) (Fig. 10C).

3.7. Influence of transport timescales on the anoxia risk

The pattern of average flushing times estimated by the hydrodynamic model for June and July 2023 showed shorter water retention times in the central and southeastern lagoon areas (~5.0 d) compared to the northern and northwestern zones of the lagoon (8.0–10.0 d) (Fig. 11 and Table 4). The calculated flushing times at each station during every month of 2023 exhibited a similar trend as during summer. A minimum and a maximum T_f value of 2.7 d and 10.4 d were obtained in November at St.6 and in May at St.3, respectively (Fig. 2S - Supplementary material). On the other hand, vertical exchange times

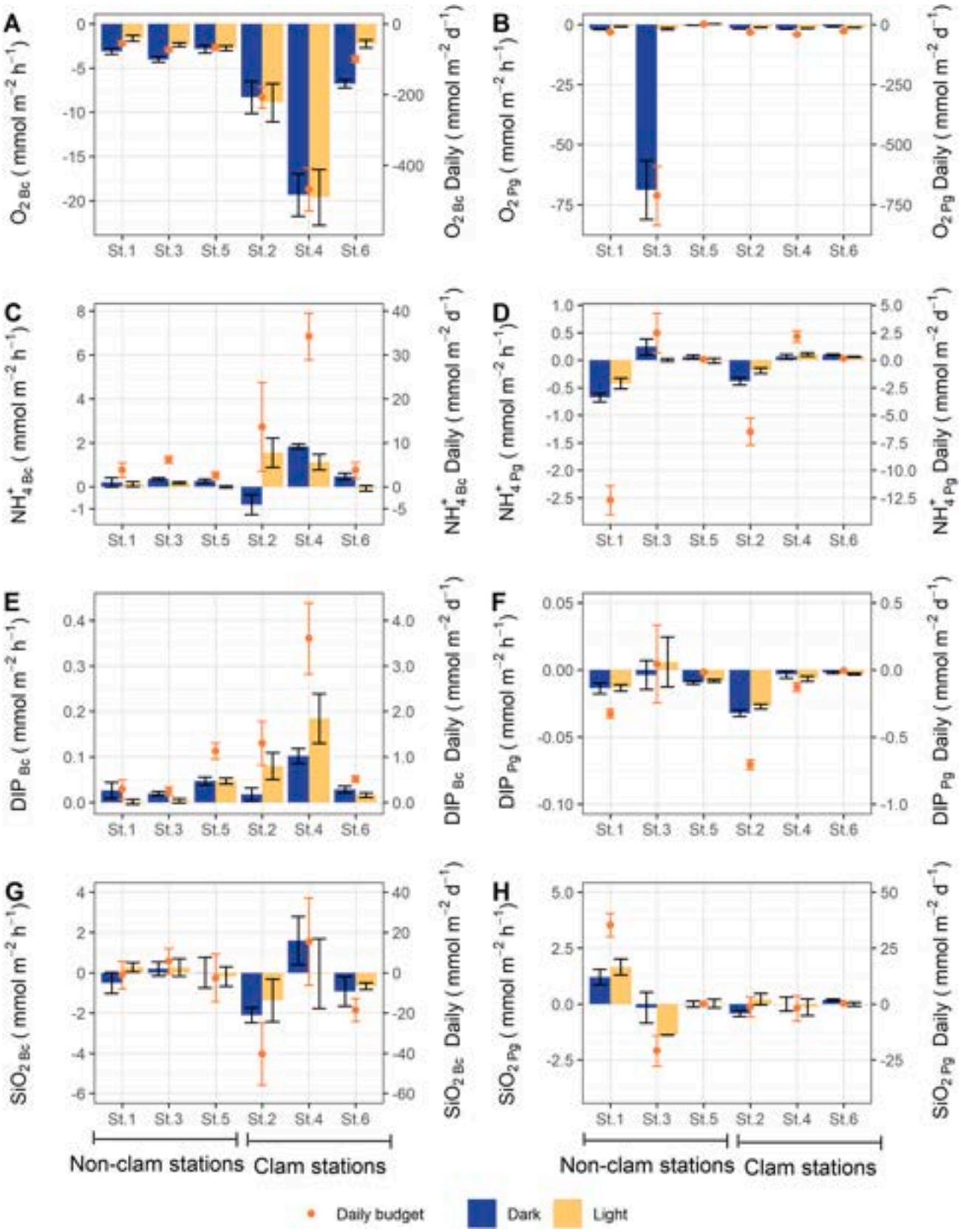

Fig. 5. Average light, dark and daily benthic and pelagic fluxes measured in the lab at six stations in the SG Lagoon during summer 2023. Benthic fluxes: (**A**) O_{2Bc}, (**C**) NH_{Bc}^{+}, (**E**) DIP_{Bc} and (**G**) SiO_{2Bc}. Pelagic fluxes: (**B**) O_{2Pg}, (**D**) NH_{Pg}^{+} (**F**) DIP_{Pg} and (**H**) SiO_{2Pg}. Light (NP, net production), dark (RE, respiration) and net daily fluxes were calculated multiplying NP and RE by the corresponding number the light and dark hours in a day. (Stations without clams: St.1, St.3 and St.5; Stations with clams St.2, St. 4 and St.6). (Average ± standard error, n = 6).

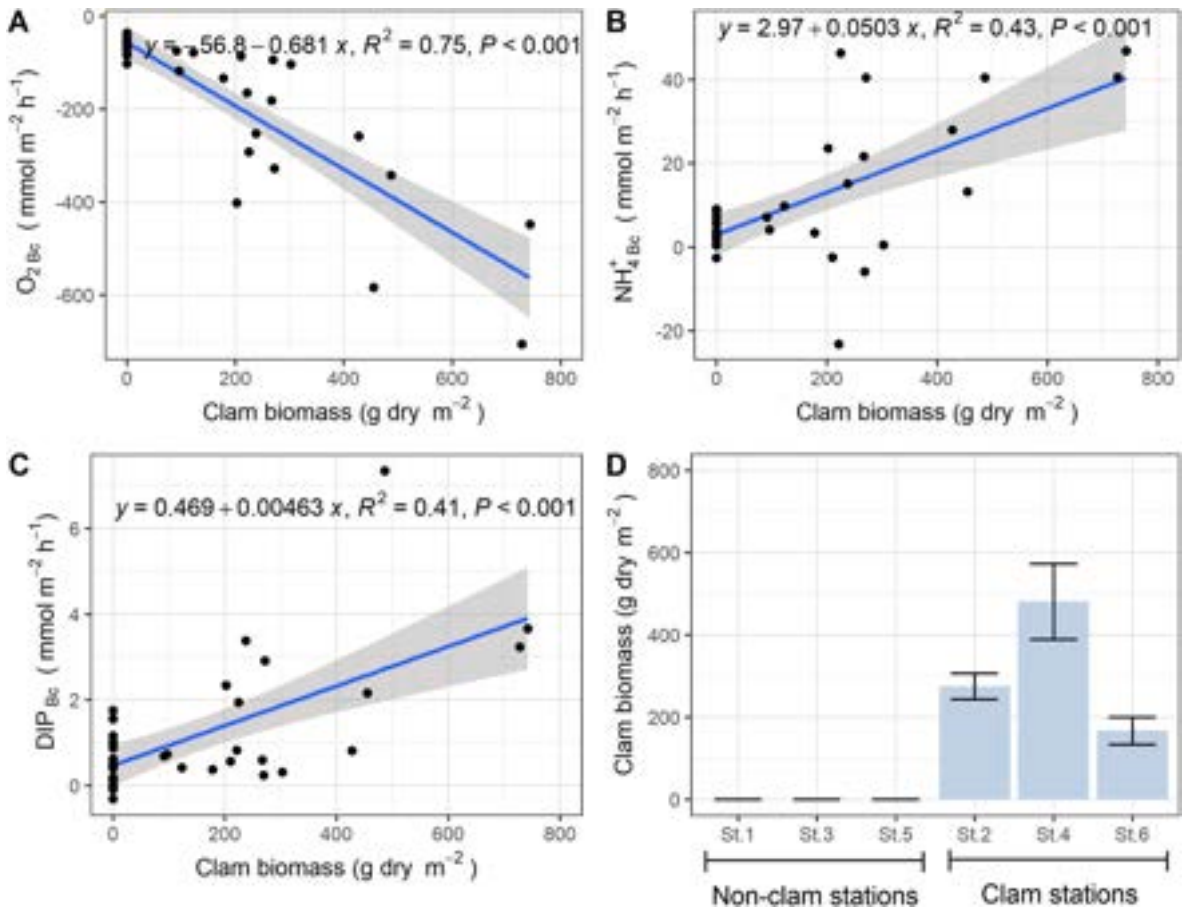

Fig. 6. Scatter plot between **(A)** O_{2BC}, **(B)** NH_{BC}^{+}, **(C)** DIP_{BC} vs clam biomass, average clam dry weight at stations (St.2, St.4 and St.6) **(D)** in the SG Lagoon during summer 2023. Pearson correlation was used to obtain the p and R^2 values in linear regressions (n = 36). The grey lines indicate 95 % confidence intervals.

estimates from Eq. (11) had a variation range from around 5 min at St.2 and St.6–104 min at the deepest station (St.3). As the vertical transport timescales (T_V) were around three orders of magnitude shorter than the horizontal transport timescales (T_f) in the SG lagoon (Table 4), the vertical mixing is the dominant transport process supporting DO replacement in the lagoon. The estimated average values of γ_V ($\gamma_V > 1$) during summer 2023 were consistent with the DO_{WC} concentrations in the water column (Fig. 2C).

4. Discussion

4.1. Drivers with the potential to trigger anoxia events in the SG lagoon

Our calculations suggest that the timescales to anoxia onset can be 2 to 10 times faster at clam farming stations and at the deepest station than at shallow non-farmed stations. While the anoxia onset in clams farming stations is mainly due to respiration by clam biomass, at the deepest part of the lagoon it can also be modulated by the water column respiration. The shorter biogeochemical timescales indicated faster rates of both O_2 consumption and nutrient replenishment (NH_4^+ and DIP) to the pelagic compartment in farming areas. During summer, in the SG, such fast dynamics can be counteracted by the O_2 supply hydrodynamically driven by the vertical exchange timescales ($\gamma_V > 1$), but not by horizontal transport timescales ($\gamma < 1$) (Figs. 10D and 11 and Table 4). A different situation may occur during extreme events like macroalgal blooms that prevent both vertical and horizontal transport mechanisms, leading to oxygen depletion, as reported by Viaroli et al. (2006).

Hypoxia and/or anoxia occurrence is considered a major global stressor impacting estuarine and marine ecosystems, and several globally widespread records suggest a rapid increase in their frequency, magnitude and extent over the last century (Diaz, 2001; Diaz and Rosenberg, 2008; Zhang et al., 2010; Breitburg et al., 2018). The risk of hypoxia/anoxia is currently one of the most relevant economic and environmental issues in estuarine and coastal marine systems, and it is most likely accelerated by human activities and climate change, potentially leading to seasonal chronic O_2 deficiency in many aquatic ecosystems in the coming decades (Schmidt et al., 2017; Rigaud et al., 2021; Le Ray et al., 2023). Therefore, the understanding of the complex interplay of physical and biogeochemical factors that promote hypoxia/anoxia is essential for developing effective management strategies to limit deoxygenation in changing climatic and environmental conditions in coastal areas.

Our outcomes show that clam biomass was the dominant factor regulating daily benthic fluxes, while clam biomass and NH_{pw}^{+} were the main predictors modulating the biogeochemical timescales (T_{Anoxia}, T_{NH4} and T_{DIP}). The average daily O_{2BC} consumption and nutrient recycling (NH_{BC}^{+} and DIP_{BC}) were stimulated several folds by the clams presence, which is in accordance with results found in the SG during summer by Bartoli et al. (2001) and Nizzoli et al. (2007). Bartoli et al. (2001) estimated that in the presence of the clam *R. philippinarum* (349.4 ± 203.8 g_{dry} m^{-2}) benthic O_2 consumption and NH_4^+ and DIP recycling in the SG were stimulated by a factor of 1.8, 6.5, 4.6, respectively, as compared to sediments without clams. Nizzoli et al. (2007) reported that *R. philippinarum* biomass of 355 ± 30 g_{DW} m^{-2} and 408 ± 146 g_{dry} m^{-2} increased in June and August daily O_{2BC} consumption and NH_4^+ recycling in the SG sediment by a factor of 3.0–3.6 and 1.9–4.9, respectively, compared to control sediments. The strong influence of clams on benthic fluxes and nutrient turnover times is due to their respiration and

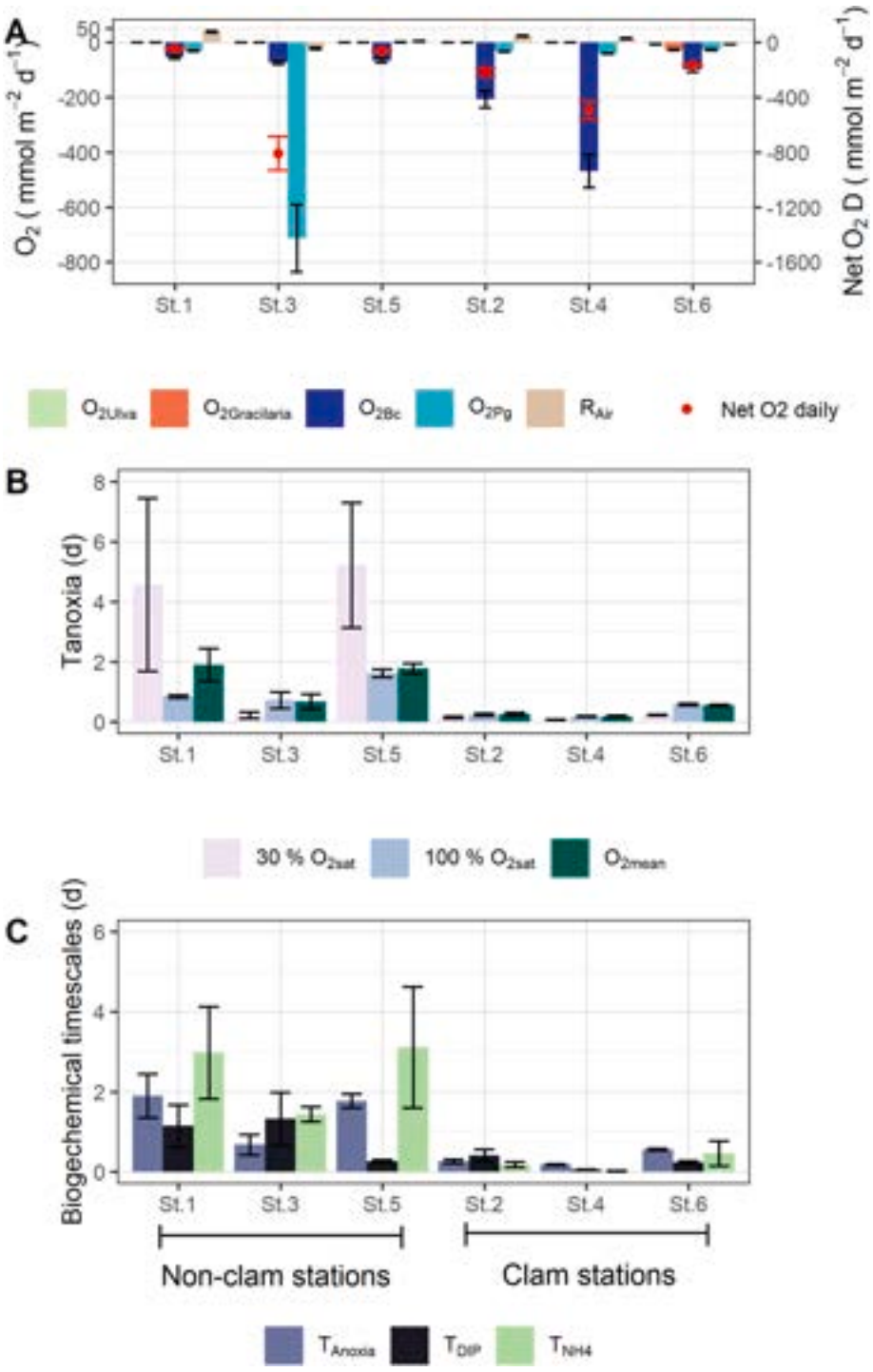

Fig. 7. Sources of consumption and supply of oxygen in the daily O_2 net consumption rate **(A)**; the effect of the reaeration on timescale of anoxia ocurrence (T_{Anoxia}) (30 % O_2 saturation, 100 % O_2 saturation and O_2 mean: O_2 concentration measured during sampling) **(B)**; and biogeochemical timescales (T_{Anoxia} (O_2mean), T_{DIP} and T_{NH4}) at the six stations in the SG Lagoon during summer 2023 (Stations without clams: St.1, St.3 and St.5; Stations with clams St.2, St. 4 and St.6.) **(C).** (Average ± standard error, n = 6).

excretion rates that are major components of their bioenergetic (Nie et al., 2017). For instance, Murphy et al. (2016) estimated that around 15–30 % of the C and N assimilated by the clam *Mercenaria mercenaria* is subsequently respired and excreted. The high bacterial biodegradability of clam's feces and pseudofaeces can in turn favor their fast mineralization, with a positive feedback on O_2 consumption and nutrient recycling (Bartoli et al., 2001; Viaroli et al., 2006). Indeed, the large influence of clams on the recycling of NH_4^+ more than of DIP could be explained by the ammonification of labile and N-rich organic matter from excretion (Nizzoli et al., 2007; Nicholaus and Zheng, 2014; Murphy et al., 2016). On the other hand, nutrients regeneration and O_2 consumption rate across the sediment-water interface are also stimulated by bioturbation activities (reworking and bioirrigation) through burrow construction in the sediments, feeding, crawling and burial by clams (Nicholaus and Zheng, 2014). Macrofauna bioturbation enhances the oxidation of anoxic sediments and increases the aerobic microbial

Table 4
Average values of timescales of anoxia onset, horizontal and vertical transport and anoxia risk in the SG Lagoon during June and July 2023.

Station	T_{Anoxic} (d)[a]	T_f (d)[b]	γ[c]	K_V ($m^2\ s^{-1}$) x 10^{-4}	Depth (m)	T_V (d) x 10^{-3}[d]	γ_V[e]	T'_{Anoxia} (d)[f]
St.1	1.9 ± 0.6	8.2 ± 0.5	0.2	3.7 ± 1.2	0.52	9.2 ± 2.7	206.4	0.8 ± 0.1
St.2	0.3 ± 0.1	7.6 ± 0.3	0.04	3.4 ± 0.8	0.3	3.2 ± 0.7	84.6	0.2 ± 0.0
St.3	0.7 ± 0.3	8.2 ± 0.9	0.1	3.9 ± 1.5	1.47	72.0 ± 25.9	9.5	0.7 ± 0.3
St.4	0.2 ± 0.0	5.5 ± 0.2	0.03	2.8 ± 1.2	0.47	10.0 ± 3.7	18.4	0.2 ± 0.0
St.5	1.8 ± 0.2	5.5 ± 0.4	0.3	2.8 ± 1.3	0.5	13.0 ± 6.2	141.0	1.6 ± 0.1
St.6	0.6 ± 0.0	4.9 ± 0.4	0.1	5.4 ± 1.9	0.4	3.8 ± 1.2	146.6	0.6 ± 0.0

[a] Calculated considering the O_2 consumption within the water column and sediments and the contribution of reaeration.
[b] Calculated as e-folding flushing time.
[c] Comparison between timescales of anoxia onset and horizontal transport (flushing time).
[d] Estimated as the square of the water column depth divided by vertical turbulent diffusion coefficient.
[e] Comparison between timescales of anoxia onset and vertical transport.
[f] Calculated considering only the O_2 consumption within the water column and sediments as Fennel and Testa (2019) and Shen and Quin (2024).

activity over the anaerobic one (Benelli et al., 2025).

The higher recycling of NH_4^+ and DIP in clam stations was consistent with the low amounts of TOC and TN in the sediment and DIP_{pw} and NH_{4pw}^+ concentrations in the pore water compared to non-farmed stations (Figs. 3 and 4). The farmed area located near St.2 had more chemically reduced conditions than the other two clam stations due to higher concentration of $Fe(II)_{pw}$ and DIP_{pw}. This is probably explained by a higher prevalence of the terrestrial material (TOC_{terr}) from northwestern than from the central and southeastern areas. The St.2 had around 2–3 times more TOC_{terr} than St.4 and St.6 during the sampling. On the other hand, the higher $Fe(II)_{pw}$:DIP_{pw} at St.6 suggests a potentially large buffer capacity of these sediments as traps of DIP_{pw} via precipitation with Fe (III) oxyhydroxides (Fig. 3I ad Fig. 4H) as suggested by Benelli et al. (2025). Our results did not show an enrichment in organic matter and elevated pore water nutrient concentration by clam activity because we analyzed the spatial variation considering the heterogeneity of the lagoon and we did not consider temporal variations. However, studies that have assessed both the spatial and temporal impacts during the clam farming cycle have found an increase in chemically reduced conditions in sediments along with a clam production cycle (Nizzoli et al., 2007). The $\delta^{13}C$ signatures of superficial sediments indicated a difference in the nature and origin of organic matter in the SG Lagoon. The spatial trend of $\delta^{13}C$ values showed an increase of their signatures (less negative values) from northwestern (St.1 and St.2) towards central and southeastern areas (St.3, St.4, St.5 and St.6). This suggests that the Po di Volano River and freshwater channels probably have a higher contribution of terrestrial material (e.g., fertilizers from agricultural activities, wastewaters, etc.) than the Po di Goro River. This spatial pattern is in agreement with the results of trophic state (Fig. 2) and the results reported by Bianchini et al. (2015) and Natali and Bianchini (2018).

The negative correlation of clam biomass with TOC, NH_{4pw}^+, DIP_{pw}, H_2S_{pw}, SiO_{2pw} and $Mn(II)_{pw}$ suggests that the sediment quality in clam rearing areas in the SG should be maintained with low organic matter content and pore water nutrient concentrations (Figs. 8, 9 and 1S). Other studies suggest that sediments with higher sand content are a better substratum than muddy bottom for clams (Melià et al., 2003; Vincenzi et al., 2006). The low levels of TOC (0.09–0.57 %) and TN (lower than detection limits) in the three stations with clams are likely due to marine water flushing that displaces to low-energy areas the large inputs of labile biodeposits produced by clams (Figs. 1S and 3B). As the sedimentary features and pore water concentrations were highly correlated, RDA results showed that NH_{4pw}^+ along with clam biomass were the main predictors of biogeochemical timescales (Fig. 9B). The smaller timescales occur in clam areas with low NH_{4pw}^+. The strong influence of clams on benthic N cycling, and particularly on NH_4^+ production and its efflux, has been reported by Nizzoli et al. (2007) and Murphy et al. (2016).

Generally, the O_2 consumption rates in shallow coastal lagoons are mainly driven by the benthic rather than the pelagic system (Fennel and Testa, 2019; Rigaud et al., 2021). We investigated the spatial heterogeneity of the benthic and pelagic O_2 dynamics as well as their contributions to the whole O_2 consumption rates and the establishment of anoxia in the SG (Table 3 and Fig. 7). While the anoxia onset was driven by clam biomass in farming areas, in the vicinity of St.3 it was also modulated by water column respiration, even though the St.3 had a low TOC_{terr} and a high accumulation of reduced chemical species in surface sediments (Figs. 3 and 4). The St.3 was located in the lagoon deepest zone (~3–5 times deeper than other stations) and had the highest Chl-a concentrations in the water column suggesting that the pelagic biomass respiration was quantitatively comparable to the sediment respiration at the other stations (Table 3).

4.2. *Do anoxia onset timescales versus transport timescales suggest a risk of O_2 depletion in the SG lagoon?*

Our results show that the anoxia risk in the SG Lagoon can be counteracted by the vertical mixing ($\gamma_V > 1$), but not by horizontal transport ($\gamma < 1$) as vertical exchange times (0.003–0.072 d) were always shorter than timescales of anoxia onset (0.19–1.9 d) (Figs. 10A and 11, Table 4). These findings are consistent with Shen and Qin (2024), who demonstrated that the shortest timescale between vertical and horizontal transport determines the DO replenishment and is the dominant factor physically controlling DO dynamics in estuaries. With the average values of γ_V estimated using T_V, we obtained a more accurate representation of the DO_{WC} conditions in the water column as compared to γ values estimated using T_f (Fig. 2C–Table 4). This highlights the importance of considering both vertical and horizontal transport to understand the DO dynamics in an estuary using timescale analysis. The pattern of flushing time computed in the SG during summer 2023 by averaging the months of June and July (Fig. 11) aligns with the results of Maicu et al. (2018, 2021). The riverine inputs of the Po di Volano and Po di Goro are the main drivers of the estuarine circulation of the lagoon. The highest average T_f value in the northwestern area was due to the lower discharge of Po di Volano compared to Po di Goro during the simulation period. On the other hand, mean values of Ks used to estimate T_V are consistent with values for shallow lagoons (Cousins et al., 2010).

The importance of the vertical exchange in the O_2 replenishment is also evident by the effect of reaeration on T_{Anoxia} (Fig. 7B). Reaeration had a strong effect on the re-oxygenation in shallow non-farmed areas (St.1 and St.5) for the scenario considering a 30 % O_2 saturation in the water column. However, the reaeration effect could be even higher in the SG lagoon considering the large variations of the O_2 saturation in the SG, between 200 % in the afternoon and 0 % in the night (Viaroli et al., 2006).

The biogeochemical and transport timescales analysis proved to be a powerful method to quantify the DO conditions and understand the intricate interplay between O_2 consumption and physical processes that can potentially trigger anoxic events in a complex shallow eutrophic lagoon with clam's aquaculture. Indeed, the SG lagoon did not show anoxic conditions during the sampling. However, the average values of

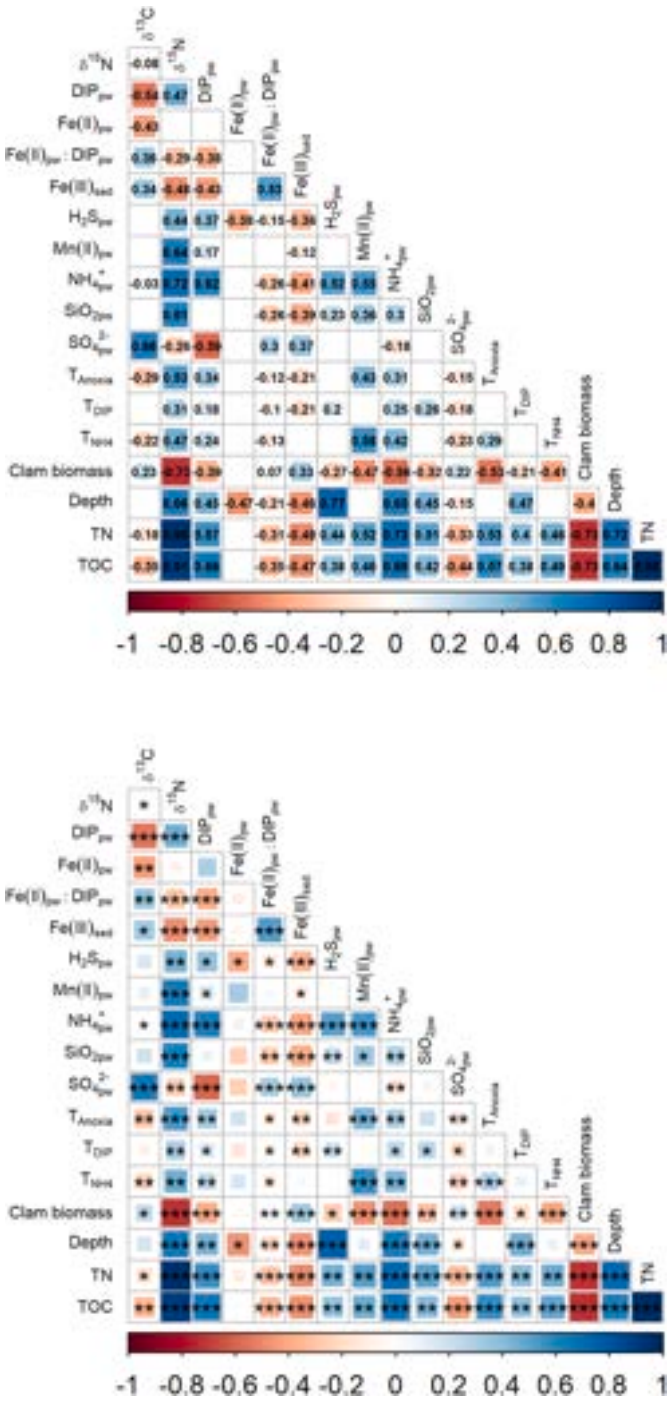

Fig. 8. Pearson correlation coefficients (r) between biogeochemical timescales (T_{NH4} and T_{DIP} and T_{Anoxia}) with sedimentary features and pore water concentrations in the benthic system **(A)**, and statistical significance level: p – value < 0.0001 = ***, p-value <0.01 = ** and p-value<0.05 = * **(B)**.

γ_V at the deepest station (St.3) and at the greatest clam biomass station (St.4) were around 5 to 20 times lower than at the other stations (Table 4 and Fig. 10D). This suggests for instance that an increase in clam biomass above the average value of 481.05 ± 91.54 g $_{DW}$ m^{-2} at St.4 or an increase of Chl-a above the mean value of 56.77 ± 12.42 μg L^{-1} at St. 3 may rapidly turn specific lagoon areas anoxic. The dynamics of OD_{WC} in shallow eutrophic coastal lagoons are demonstrated to fluctuate rapidly during the day, dropping from oversaturation to hypoxia/anoxia within a few hours during the night (D'Autilia et al., 2004; Xu and Xu, 2016; Shadrin et al., 2023). The O_2 dynamic in shallow eutrophic lagoon

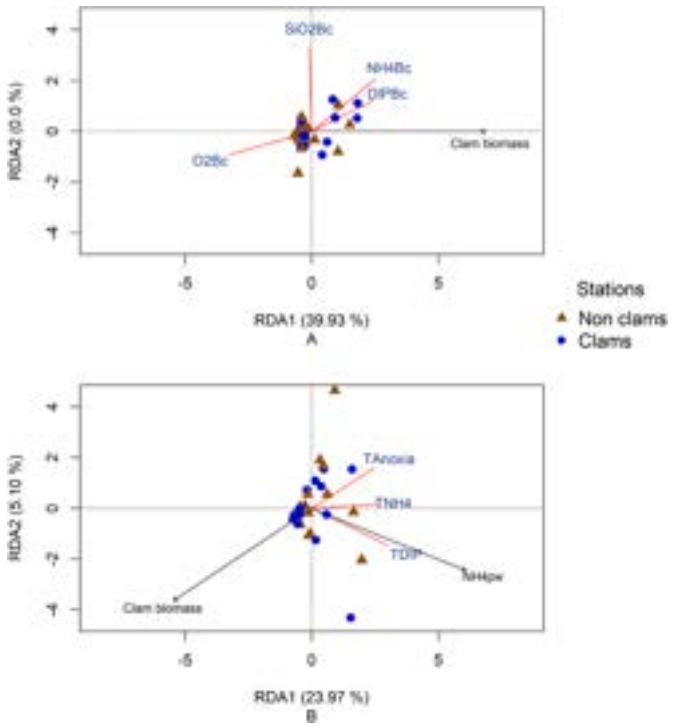

Fig. 9. RDA analysis triplots showing the main environment parameters driving **(A)** daily benthic fluxes (O_{2Bc}, NH_{4Bc}^{+}, DIP_{Bc} and SiO_{2Bc}) and **(B)** biogeochemical timescales (T_{NH4}, T_{DIP} and T_{Anoxia}) in the SG Lagoon during summer 2023. The analysis is based on scaling 2 method. The cosine of angles between response variables and explanatory variables, as well as the cosine of angles of the same response and explanatory variables reflect their linear correlation coefficients (e.g., no correlation: cos (90°) = 0, strong positive correlation: cos (0°) = 1, positive correlation: cos (30°) = 0.87, strong negative correlation: cos (180°) = −1.

with clam's aquaculture also evolves through complex feedback loops. For instance, another factor contributing to the variability in water quality and DO_{WC} at farming stations is the filtration capacity of clams, which also depends on their relative abundance. A more accurate estimation of γ_V in the SG requires the implementation of high-frequency O_2 measurements in the water column and a coupled 3D hydrodynamic-ecological model. Such implementation would allow improving the quantification of all processes and understanding the synergy among them (e.g., changes in water quality of rivers, wind stress, clam filtration rates, etc.) in the context of hourly and not daily O_2 budgets (D'Autilia et al., 2004; Spillman et al., 2008).

The anoxia risk assessment of mollusk aquaculture in shallow, microtidal coastal lagoons is a complex issue, as O_2 concentrations in very productive coastal ecosystems are highly variable. They depend on the interplay of hydrodynamic conditions and biogeochemical processes with site-specific features and forcing events, acting over a wide range of temporal and spatial scales. Consequently, the timescales taken into account in the present work integrated multiple biogeochemical and physical processes, measured and modeled (O_2 and nutrients daily fluxes in benthic and pelagic compartment, reaeration coefficient, vertical and horizontal transport). On the other hand, the RDA was used to assess the influence of a large number of potentially important environmental factors, and to identify the main predictors of both daily fluxes and timescales. Finally, the spatial representation of the timescales in GIS allowed to obtain a better understanding of timescales of anoxia onset and nutrient recycling, and the potential risk of anoxia, considering the large spatial heterogeneity of the lagoon.

It is worth noting that the spatial representation of biogeochemical timescales and γ_V in GIS provides essential information that can be used by decision makers to develop effective management strategies and

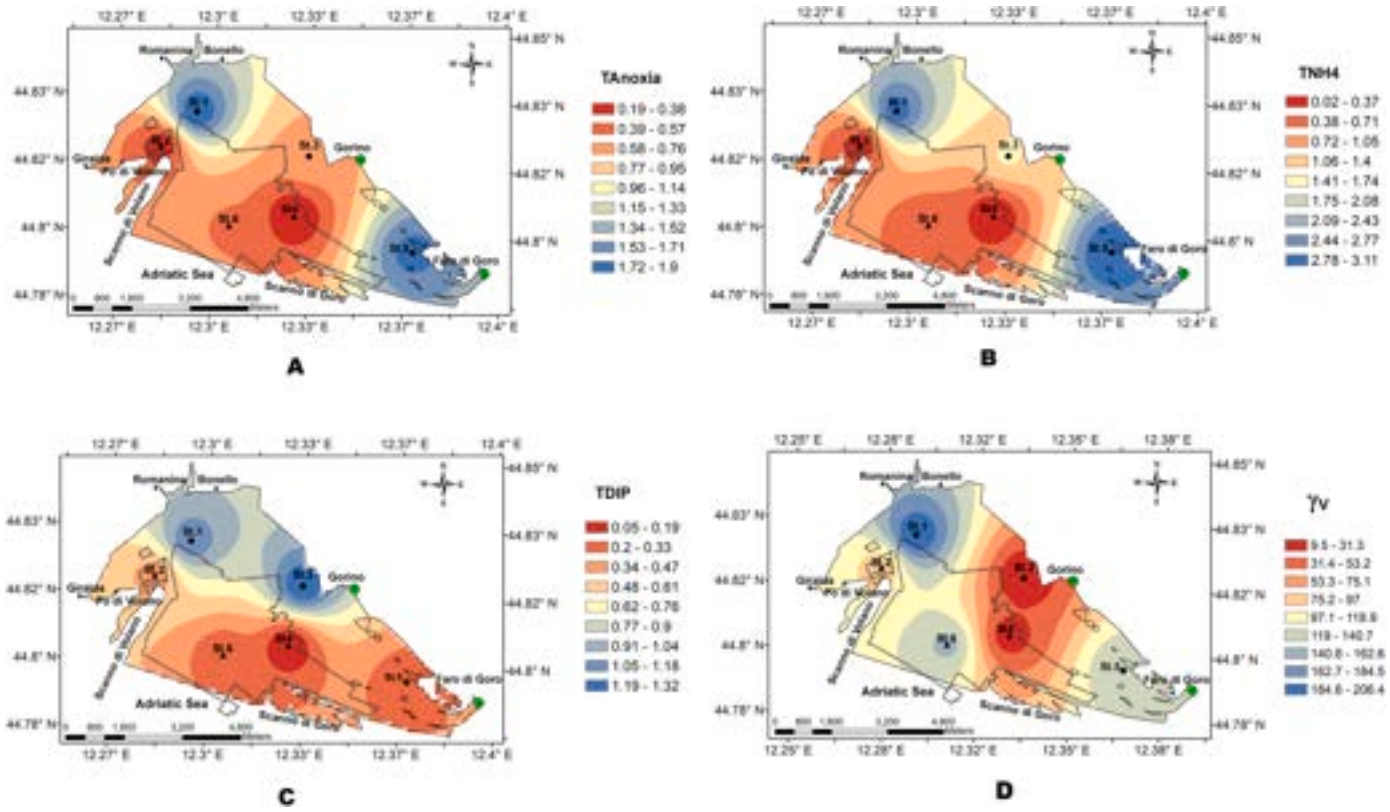

Fig. 10. Spatial distribution of timescale anoxia occurrence (T_{Anoxia}) **(A)**, NH_{BC}^{+} turnover times (T_{NH4}) **(B),** DIP_{BC} turnover (T_{DIP}) **(C),** and γ_V, which relates the timescale of anoxia onset (T_{Anoxia}) to the vertical exchange time (T_V) **(D)** in the SG Lagoon during summer 2023.

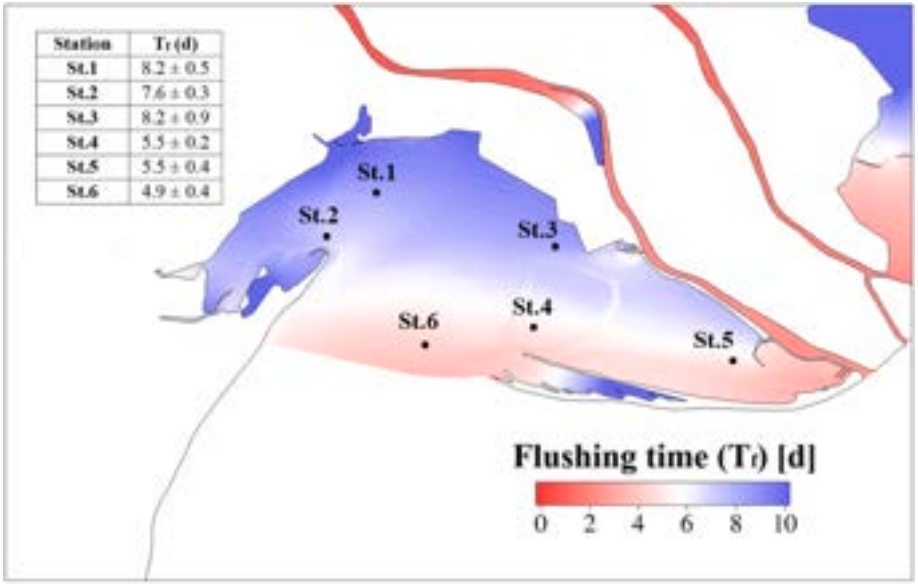

Fig. 11. Average flushing time (T_f) estimated during June and July 2023 in the SG lagoon by the SHYFEM model.

adaptation to changing climatic and environmental conditions in the SG lagoon. The increasingly severe and prolonged episodes of summer heat waves in the Mediterranean region can intensify the frequency of anoxia risk events in the SG Lagoon as a result of the drastic decrease in water circulation patterns and the increase of retention times due to the reduction of river discharge and inflow. Furthermore, higher temperatures and salinities diminish O_2 solubility and increase O_2 consumption rates, therefore reducing O_2 concentration in the water column. The interactive combination of these effects would suggest a reduction of the density of farmed clams in areas under major risk to avoid economic losses and impacts to the benthic system in terms of biodiversity and functioning. Indeed, deoxygenation events often result in build-up of toxic free sulphides and short circuits of both N and P removal/retention benthic mechanisms, with positive feedback for eutrophication.

This work is not conclusive as unpredictable changes in both pelagic and benthic diversity and abundance of organisms, including

opportunistic invasive species, are expected along extreme events related to climate change. We strongly suggest increasing the frequency of monitoring activities in coastal lagoons in this period of transition to a new climatic regime, and to include, besides traditional parameters, the measurements of communities and processes. In the present study the clearance rate of clams in the different cultivated areas and the phytoplankton production were not measured. In situ filtration rate is an important process to characterize how clams control phytoplankton growth, and to couple suspended particle-associated nutrient removal, nutrient regeneration from sediment, and nutrient retention in buried biodeposits. In situ evaluation of phytoplankton production is important as well, as it provides information on the net budget of microalgal biomass, resulting from filtration, in situ growth, freshwater input and marine export. Future studies in the SG lagoon should include these measurements.

CRediT authorship contribution statement

Diana M. Arroyave Gómez: Writing – review & editing, Writing – original draft, Visualization, Methodology, Investigation, Formal analysis, Data curation, Conceptualization. **Leonardo Morini:** Writing – review & editing, Methodology. **Samuele Pagani:** Writing – review & editing, Methodology. **Sara Benelli:** Writing – review & editing, Methodology. **Monia Magri:** Writing – review & editing, Methodology. **Georg Umgiesser:** Writing – review & editing, Software. **Luis Germano Biolchi:** Writing – review & editing, Software. **Giuseppe Castaldelli:** Writing – review & editing, Funding acquisition, Conceptualization. **Marco Bartoli:** Writing – review & editing, Supervision, Funding acquisition, Conceptualization.

Declaration of competing interest

The authors declare that they have no known competing financial interests or personal relationships that could have appeared to influence the work reported in this paper.

Acknowledgements

This work was supported by the Emilia Romagna Region through the project "Valutazione e mappatura della produttività ai fini dell'acquacoltura di molluschi bivalvi della Sacca di Goro e del tratto di costa dal Lido di Volano al Lido delle Nazioni". It has also benefited from the equipment and framework of the COMP HUB and COMP-R Initiatives, funded by the 'Departments of Excellence' program of the Italian Ministry for University and Research (MUR, 2018–2022 and MUR, 2023–2027). We are thankful with ARPAE and with Dr. Christian Ferrarin for the possibility of running the hydrodynamic simulations of the Sacca di Goro for the year 2023 on its server. We are also grateful to three anonymous reviewers for their accurate and constructive comments.

Appendix A. Supplementary data

Supplementary data to this article can be found online at https://doi.org/10.1016/j.jenvman.2025.126955.

Data availability

The authors don't want to share the data because data will use to apply another methodology to assess suitable areas for clam farming

References

APHA (American Public Health Association), 2012. Standard Methods for the Examination of Water and Wastewater, twenty-second ed. Washington, D.C., USA.

Arroyave Gómez, D.M., Gallego Suárez, D., Bartoli, M., Toro-Botero, M., 2020. Spatial and seasonal variability of sedimentary features and nitrogen benthic metabolism in a tropical coastal area (Taganga Bay, Colombia Caribbean) impacted by a sewage outfall. Biogeochemistry 150 (1), 85–107. https://doi.org/10.1007/s10533-020-00689-0.

Bartoli, M., Nizzoli, D., Viaroli, P., Turolla, E., Castaldelli, G., Fano, E.A., Rossi, R., 2001. Impact of Tapes philippinarum farming on nutrient dynamics and benthic respiration in the Sacca di Goro. Hydrobiologia 455, 203–212. https://doi.org/10.1023/A:1011910422400.

Benelli, S., Janas, U., Magri, M., Kendzierska, H., Arroyave Gómez, D.M., Bartoli, M., 2025. Bio-irrigation promotes reactive phosphorus recycling in an oxidized sedimentary environment. Estuaries Coasts 48 (1). https://doi.org/10.1007/s12237-024-01450-8.

Bianchini, G., Natali, C., Fogli, R., Antisari, L.V., 2015. Preliminary Notes on C-N Pools in Subaqueous Soils From the Sacca Di Goro Coastal Lagoon (Po Delta, Northern Italy). EQA - Int. J. Environ. Qual. 19, 45–54. https://doi.org/10.6092/issn.2281-4485/5800.

Bianchini, G., Brombin, V., Carlino, P., Mistri, E., Natali, C., Salani, G.M., 2021. Traceability and authentication of manila clams from north-western adriatic lagoons using C and N stable isotope analysis. Molecules 26. https://doi.org/10.3390/molecules26071859.

Biolchi, L.G., Valentini, A., Unguendoli, S., Umgiesser, G., Ferrarin, C., 2025. Marine Climate Downscaling in Coastal and Transitional Areas: the Case of the Emilia-Romagna Region in the Northwest Adriatic Sea (submitted to Frontiers).

Breitburg, D., Levin, L.A., Oschlies, A., Grégoire, M., Chavez, F.P., Conley, D.J., et al., 2018. Declining oxygen in the global ocean and coastal waters. Science 359. https://doi.org/10.1126/science.aam7240.

Clementi, E., Aydogdu, A., Goglio, A.C., Pistoia, J., Escudier, R., Drudi, M., Pinardi, N., 2021. Mediterranean sea physical analysis and forecast (CMEMS MED-Currents, EAS6 system)(version 1). Copernicus Monitoring Environment Marine Service (CMEMS) 10, 405 [Data set].

Cline, J.D., 1969. Spectrophometric determination of hydrogen sulfide in natural waters. Limnol. Oceanogr. 14, 454–458. https://doi.org/10.4319/lo.1969.14.3.0454.

Cousins, M., Stacey, M.T., Drake, J.L., 2010. Effects of seasonal stratification on turbulent mixing in a hypereutrophic coastal lagoon. Limnol. Oceanogr. 55, 172–186. https://doi.org/10.4319/lo.2010.55.1.0172.

Cucco, A., Umgiesser, G., 2006. Modeling the Venice Lagoon residence time. Ecol. Model. 193, 34–51. https://doi.org/10.1016/j.ecolmodel.2005.07.043.

Cutrim, M.V.J., Ferreira, F.S., Duarte dos Santos, A.K., Cavalcanti, L.F., Araújo, B. de O., de Azevedo-Cutrim, A.C.G., Furtado, J.A., Oliveira, A.L.L., 2019. Trophic state of an urban coastal lagoon (northern Brazil), seasonal variation of the phytoplankton community and environmental variables. Estuar. Coast Shelf Sci. 216 (August 2018), 98–109. https://doi.org/10.1016/j.ecss.2018.08.013.

D'Autilia, R., Falcucci, M., Hull, V., Parrella, L., 2004. Short time dissolved oxygen dynamics in shallow water ecosystems. Ecol. Model. 179, 297–306. https://doi.org/10.1016/j.ecolmodel.2004.02.009.

Dalsgaard, T., Nielsen, L.P., Brotas, V., et al., 2000. Protocol handbook for nitrogen cycling in estuaries. In: Dalsgaard, T. (Ed.), Issue a Project Under the EU Research Programme: Marine Science and Technology (MAST III). National Environmental Research Institute, Silkeborg, Denmark.

Derolez, V., Malet, N., Fiandrino, A., Lagarde, F., Richard, M., Ouisse, V., Bec, B., Aliaume, C., 2020. Fifty years of ecological changes: regime shifts and drivers in a coastal Mediterranean lagoon during oligotrophication. Sci. Total Environ. 732. https://doi.org/10.1016/j.scitotenv.2020.139292.

Diaz, R.J., 2001. Overview of hypoxia around the world. J. Environ. Qual. 30, 275–281. https://doi.org/10.2134/jeq2001.302275x.

Diaz, Robert J., Rosenberg, R., 2008. Spreading dead zones and consequences for marine ecosystems. Science 321, 926–929. https://doi.org/10.1126/science.1156401.

Druon, J.N., Schrimpf, W., Dobricic, S., Stips, A., 2004. Comparative assessment of large-scale marine eutrophication: North sea area and Adriatic Sea as case studies. Mar. Ecol. Prog. Ser. 272, 1–23. https://doi.org/10.3354/meps272001.

Fennel, K., Testa, J.M., 2019. Biogeochemical controls on coastal hypoxia. Ann. Rev. Mar. Sci 11, 105–130. https://doi.org/10.1146/annurev-marine-010318-095138.

Gammal, J., Norkko, J., Pilditch, C.A., Norkko, A., 2017. Coastal hypoxia and the importance of benthic Macrofauna communities for ecosystem functioning. Estuaries Coasts 40, 457–468. https://doi.org/10.1007/s12237-016-0152-7.

Gastaldo, T., Poli, V., Marsigli, C., Cesari, D., Alberoni, P.P., Paccagnella, T., 2021. Assimilation of radar reflectivity volumes in a pre-operational framework. Q. J. R. Meteorol. Soc. 147, 1031–1054. https://doi.org/10.1002/qj.3957.

Giovanardi, F., Vollenweider, R.A., 2004. Trophic conditions of marine coastal waters: experience in applying the trophic index TRIX to two areas of the Adriatic and Tyrrhenian seas. J. Limnol. 63, 199–218. https://doi.org/10.4081/jlimnol.2004.199.

Große, F., Greenwood, N., Kreus, M., Lenhart, H.J., Machoczek, D., Pätsch, J., Salt, L., Thomas, H., 2016. Looking beyond stratification: a model-based analysis of the biological drivers of oxygen deficiency in the North Sea. Biogeosciences 13, 2511–2535. https://doi.org/10.5194/bg-13-2511-2016.

Lacoste, É., Bec, B., Le Gall, P., Boufahja, F., Raimbault, P., Messiaen, G., et al., 2022. Benthic-pelagic coupling under juvenile oyster influence in a French Mediterranean coastal lagoon (Thau Lagoon). Estuar. Coast Shelf Sci. 267. https://doi.org/10.1016/j.ecss.2022.107779.

Lavoie, M.F., McKindsey, C.W., Pearce, C.M., Archambault, P., 2016. Influence of intertidal Manila Clam Venerupis Philippinarum Aquaculture on biogeochemical fluxes. Aquac. Environ. Interact. 8, 118–130. https://doi.org/10.3354/aei00167.

Le Ray, J., Bec, B., Fiandrino, A., Lagarde, F., Cimiterra, N., Raimbault, P., Roques, C., Rigaud, S., Régis, J., Mostajir, B., Mas, S., Richard, M., 2023. Impact of anoxia and oyster mortality on nutrient and microbial planktonic components: a mesocosm study. Aquaculture 566. https://doi.org/10.1016/j.aquaculture.2022.739171.

Legendre, P., Legendre, L., 1998. Numerical ecology, 2nd edition Dev. Environ. Model. 20. https://doi.org/10.1017/CBO9781107415324.004. *24*, 870.
Leoni, S., Dominik, J., Cassin, D., Manfè, G., Tagliapietra, D., Acri, F., Zonta, R., 2022. Sediment oxygen demand rate in a flow regulated lagoon (Venice, Italy). Front. Environ. Sci. 10, 1–16. https://doi.org/10.3389/fenvs.2022.1000665.
Li, Y., Zhang, H., Tu, C., et al., 2016. Sources and fate of organic carbon and nitrogen from land to ocean: identified by coupling stable isotopes with C/N ratio. Estuar. Coast Shelf Sci. 181, 114–122. https://doi.org/10.1016/j.ecss.2016.08.024.
Lorenzen, C.J., 1967. Determination of chlorophyll and pheo-pigments: spectrophotometric equations. Limnol. Oceanogr. 12, 343–346. https://doi.org/10.4319/lo.1967.12.2.0343.
Lovley, D.R., Phillips, E.J.P., 1987. Rapid assay for microbially reducible ferric iron in aquatic sediments. Appl. Environ. Microbiol. 53, 1536–1540. https://doi.org/10.1128/aem.53.7.1536-1540.1987.
Lu, G.Y., Wong, D.W., 2008. An adaptive inverse-distance weighting spatial interpolation technique. Comput. Geosci. 34, 1044–1055. https://doi.org/10.1016/j.cageo.2007.07.010.
Lucas, L.V., Deleersnijder, E., 2020. Timescale methods for simplifying, understanding and modeling biophysical and water quality processes in coastal aquatic ecosystems: a review. Water 12. https://doi.org/10.3390/w12102717.
Magri, M., Benelli, S., Bonaglia, S., Zilius, M., Castaldelli, G., Bartoli, M., 2020. The effects of hydrological extremes on denitrification, dissimilatory nitrate reduction to ammonium (DNRA) and mineralization in a coastal lagoon. Sci. Total Environ. 740, 140169. https://doi.org/10.1016/j.scitotenv.2020.140169.
Maicu, F., Alessandri, J., Pinardi, N., Verri, G., Umgiesser, G., Lovo, S., Turolla, S., Paccagnella, T., Valentini, A., 2021. Downscaling with an unstructured coastal-ocean model to the Goro lagoon and the Po River Delta branches. Front. Mar. Sci. 8. https://doi.org/10.3389/fmars.2021.647781.
Maicu, F., De Pascalis, F., Ferrarin, C., Umgiesser, G., 2018. Hydrodynamics of the Po river-delta-sea system. J. Geophys. Res. Ocean. 123, 6349–6372. https://doi.org/10.1029/2017JC013601.
Marinov, D., Galbiati, L., Giordani, G., Viaroli, P., Norro, A., Bencivelli, S., Zaldívar, J.M., 2007. An integrated modelling approach for the management of clam farming in coastal lagoons. Aquaculture 269, 306–320. https://doi.org/10.1016/j.aquaculture.2007.04.071.
Marinov, D., Zaldívar, J.M., Norro, A., Giordani, G., Viaroli, P., 2008. Integrated modelling in coastal lagoons: Sacca di Goro case study. Hydrobiologia 611, 147–165. https://doi.org/10.1007/s10750-008-9451-8.
Meire, L., Soetaert, K.E.R., Meysman, F.J.R., 2013. Impact of global change on coastal oxygen dynamics and risk of hypoxia. Biogeosciences 10, 2633–2653. https://doi.org/10.5194/bg-10-2633-2013.
Melià, P., Nizzoli, D., Bartoli, M., Naldi, M., Gatto, M., Viaroli, P., 2003. Assessing the potential impact of clam rearing in dystrophic lagoons: an integrated oxygen balance. Chem. Ecol. 19, 129–146. https://doi.org/10.1080/0275754031000119898.
Monsen, N.E., Cloern, J.E., Lucas, L.V., Monismith, S.G., 2002. A comment on the use of flushing time, residence time, and age as transport time scales. Limnol. Oceanogr. 47, 1545–1553. https://doi.org/10.4319/lo.2002.47.5.1545.
Mosley, L.M., Priestley, S., Brookes, J., Dittmann, S., et al., 2023. Extreme eutrophication and salinisation in the coorong estuarine-lagoon ecosystem of Australia's largest river basin (Murray-Darling). Mar. Pollut. Bull. 188. https://doi.org/10.1016/j.marpolbul.2023.114648.
Murphy, A.E., Emery, K.A., Anderson, I.C., Pace, M.L., Brush, M.J., Rheuban, J.E., 2016. Quantifying the effects of commercial clam aquaculture on C and N cycling: an integrated ecosystem approach. Estuaries Coasts 39, 1746–1761. https://doi.org/10.1007/s12237-016-0106-0.
Nasrollahzadeh, H.S., Din, Z. Bin, Foong, S.Y., Makhlough, A., 2008. Trophic status of the Iranian Caspian Sea based on water quality parameters and phytoplankton diversity. Cont. Shelf Res. 28, 1153–1165. https://doi.org/10.1016/j.csr.2008.02.015.
Natali, C., Bianchini, G., 2018. Natural vs anthropogenic components in sediments from the Po River delta coastal lagoons (NE Italy). Environ. Sci. Pollut. Res. 25, 2981–2991. https://doi.org/10.1007/s11356-017-0986-y.
Newton, A., Icely, J., Cristina, S., Brito, A., Cardoso, A.C., et al., 2014. An overview of ecological status, vulnerability and future perspectives of European large shallow, semi-enclosed coastal systems, lagoons and transitional waters. Estuar. Coast Shelf Sci. 140, 95–122. https://doi.org/10.1016/j.ecss.2013.05.023.
Nicholaus, R., Zheng, Z., 2014. The effects of bioturbation by the Venus clam Cyclina sinensis on the fluxes of nutrients across the sediment-water interface in aquaculture ponds. Aquac. Int. 22, 913–924. https://doi.org/10.1007/s10499-013-9716-8.
Nie, H., Chen, P., Huo, Z., Chen, Y., Hou, X., Yang, F., Yan, X., 2017. Effects of temperature and salinity on oxygen consumption and ammonia excretion in different colour strains of the Manila clam, Ruditapes philippinarum. Aquac. Res. 48, 2778–2786. https://doi.org/10.1111/are.13111.
Nizzoli, D., Bartoli, M., Viaroli, P., 2007. Oxygen and ammonium dynamics during a farming cycle of the bivalve Tapes philippinarum. Hydrobiologia 587, 25–36. https://doi.org/10.1007/s10750-007-0683-9.
Nizzoli, D., Welsh, D.T., Fano, E.A., Viaroli, P., 2006. Impact of clam and mussel farming on benthic metabolism and nitrogen cycling, with emphasis on nitrate reduction pathways. Mar. Ecol. Prog. Ser. 315, 151–165. https://doi.org/10.3354/meps315151.
Oksanen, J., Blanchet, F.G., Kindt, R., Legendre, P., Minchin, P.R., O'hara, R.B., Oksanen, M.J., 2013. Package 'Vegan'. *Community Ecology Package*, vol. 9, pp. 1–295.
Peña, M.a., Katsev, S., Oguz, T., Gilbert, D., 2010. Modeling dissolved oxygen dynamics and hypoxia. Biogeosciences 7, 933–957. https://doi.org/10.5194/bg-7-933-2010.
Pittaluga, F., Aleffi, I.F., Bettoso, N., Blasutto, O., Celio, M., Codarin, A., Cumani, F., Faresi, L., Guiatti, D., Orlandi, C., Zanello, A., Acquavita, A., 2022. The SHAPE project: an innovative approach to understanding seasonal and diel dissolved oxygen dynamics in the Marano and Grado lagoon (Adriatic Sea) under the WFD/2000/60/CE. J. Mar. Sci. Eng. 10. https://doi.org/10.3390/jmse10020208.
Pratihary, A.K., Naqvi, S.W.A., Naik, H., Thorat, B.R., Narvenkar, G., Manjunatha, B.R., Rao, V.P., 2009. Benthic fluxes in a tropical Estuary and their role in the ecosystem. Estuar. Coast Shelf Sci. 85, 387–398. https://doi.org/10.1016/j.ecss.2009.08.012.
Rigaud, S., Deflandre, B., Grenz, C., Cesbron, F., et al., 2021. Benthic oxygen dynamics and implication for the maintenance of chronic hypoxia and ecosystem degradation in the Berre lagoon (France). Estuar. Coast Shelf Sci. 258. https://doi.org/10.1016/j.ecss.2021.107437.
Rodrigues, L.C., Van Den Bergh, J.C.J.M., Massa, F., Theodorou, J.A., Ziveri, P., Gazeau, F., 2015. Sensitivity of Mediterranean bivalve mollusc aquaculture to climate change, Ocean acidification, and other environmental pressures: findings from a producer survey. J. Shellfish Res. 34, 1161–1176. https://doi.org/10.2983/035.034.0341.
Schlunz, B., Schneider, R.R., Muller, P.J., et al., 1999. Terrestrial organic carbon accumulation on the Amazon deep sea fan during the last glacial sea level low stand. Chem. Geol. 159, 263–281. https://doi.org/10.1016/S0009-2541(99)00041-8.
Schmidt, S., Bernard, C., Escalier, J.M., Etcheber, H., Lamouroux, M., 2017. Assessing and managing the risks of hypoxia in transitional waters: a case study in the tidal Garonne River (South-West France). Environ. Sci. Pollut. Res. 24, 3251–3259. https://doi.org/10.1007/s11356-016-7654-5.
Seitaj, D., Sulu-Gambari, F., Burdorf, L.D.W., Romero-Ramirez, A., Maire, O., Malkin, S.Y., Slomp, C.P., Meysman, F.J.R., 2017. Sedimentary oxygen dynamics in a seasonally hypoxic basin. Limnol. Oceanogr. 62, 452–473. https://doi.org/10.1002/lno.10434.
Shadrin, N., Latushkin, A., Anufriieva, E., 2023. Spatial and daily variability of oxygen balance and chlorophyll content in the Bay Sivash ecosystem, the world's largest hypersaline lagoon. Reg. Stud. in Mar. Sci. 61, 102854. https://doi.org/10.1016/j.rsma.2023.102854.
Shen, J., Qin, Q., 2024. The general relationship between mean dissolved oxygen concentrations and timescales in estuaries. Water 16, 1–13. https://doi.org/10.3390/w16070969.
Spillman, C.M., Hamilton, D.P., Hipsey, M.R., Imberger, J., 2008. A spatially resolved model of seasonal variations in phytoplankton and clam (Tapes philippinarum) biomass in Barbamarco Lagoon, Italy. Estuar. Coast Shelf Sci. 79, 187–203. https://doi.org/10.1016/j.ecss.2008.03.020.
Staehr, P.A., Bade, D., van de Bogert, M.C., Koch, G.R., Williamson, C., Hanson, P., Cole, J.J., Kratz, T., 2010. Lake metabolism and the diel oxygen technique: state of the science. Limnol Oceanogr. Methods 8, 628–644. https://doi.org/10.4319/lom.2010.8.0628.
Steppeler, J., Doms, G., Schättler, U., Bitzer, H.W., Gassmann, A., Damrath, U., Gregoric, G., 2003. Meso-gamma scale forecasts using the nonhydrostatic model LM. Meteorol. Atmos. Phys. 82, 75–96. https://doi.org/10.1007/s00703-001-0592-9.
Umgiesser, G., Canu, D.M., Cucco, A., Solidoro, C., 2004. A finite element model for the Venice Lagoon. Development, set up, calibration and validation. J. Mar. Syst. 51, 123–145. https://doi.org/10.1016/j.jmarsys.2004.05.009.
Umgiesser, G., Ferrarin, C., Cucco, A., De Pascalis, F., Bellafiore, D., Ghezzo, M., Bajo, M., 2014. Comparative hydrodynamics of 10 Mediterranean lagoons by means of numerical modeling. J. Geophys. Res.: Ocean 119, 2212–2226. https://doi.org/10.1002/2013JC009512.
Umgiesser, G., Zemlys, P., Erturk, A., Razinkova-Baziukas, A., Mezine, J., Ferrarin, C., 2016. Seasonal renewal time variability in the Curonian Lagoon caused by atmospheric and hydrographical forcing. Ocean Sci. 12, 391–402. https://doi.org/10.5194/os-12-391-2016.
Valentini, A., Alessandri, J., Maicu, F., Turolla, S., Lovo, S., 2019. Golfem a Finite Element Model for the Management of the Goro Lagoon ,. Italy. EGU General Assembly Conference Abstracts, 15436.
Viaroli, P., Giordani, G., Bartoli, M., Naldi, M., Azzoni, R., Nizzoli, D., Ferrari, I., Comenges, J.M.Z., Bencivelli, S., Castaldelli, G., Fano, E.A., 2006. The Sacca di Goro lagoon and an arm of the Po River. Handb. Environ. Chem. 5 (PART H), 197–232. https://doi.org/10.1007/698-5-030. *Volume* 5: Water Pollution.
Villnäs, A., Norkko, J., Lukkari, K., Hewitt, J., Norkko, A., 2012. Consequences of increasing hypoxic disturbance on benthic communities and ecosystem functioning. PLoS One 7. https://doi.org/10.1371/journal.pone.0044920.
Vincenzi, S., Caramori, G., Rossi, R., De Leo, G.A., 2006. Estimating clam yield potential in the Sacca di Goro lagoon (Italy) by using a two-part conditional model. Aquaculture 261, 1281–1291. https://doi.org/10.1016/j.aquaculture.2006.08.014.
Vollenweider, R.A., Giovanardi, F., Montanari, G., Rinaldi, A., 1998. Characterization of the trophic conditions of marine coastal waters with special reference to the NW Adriatic Sea: proposal for a trophic scale, turbidity and generalized water quality index. Environmetrics 9, 329–357. https://doi.org/10.1002/(SICI)1099-095X(199805/06)9:3<329::AID-ENV308>3.0.CO;2-9.
Wanninkhof, R., 1992. Relationship between wind speed and gas exchange over the ocean. J. Geophys. Res. 97, 7373–7382. https://doi.org/10.1029/92JC00188.
Wei, T., Simko, V., Levy, M., Xie, Y., Jin, Y.J., Zemla, J., 2017. R package "corrplot". Statistician 56, 316–324. https://github.com/taiyun/corrplot.
Weiss, R.F., 1970. The solubility of nitrogen, oxygen and argon in water and seawater. Deep-Sea Res. Oceanogr. Abstr. 17, 721–735. https://doi.org/10.1016/0011-7471(70)90037-9.
Wickham, M.H., Chang, W., Wickham, M.H., 2016. Package "ggplot2". Create elegant data visualizations using the grammer of graphics. Version 2 (1), 1–89.

Xu, Z., Xu, Y.J., 2016. A deterministic model for predicting hourly dissolved oxygen change: development and application to a shallow eutrophic lake. Water 8. https://doi.org/10.3390/w8020041.

Zhang, J., Gilbert, D., Gooday, A.J., Levin, L., et al., 2010. Natural and human-induced hypoxia and consequences for coastal areas: synthesis and future development. Biogeosciences 7, 1443–1467. https://doi.org/10.5194/bg-7-1443-2010.

Zhou, J., Wu, Y., Zhang, J., et al., 2006. Carbon and nitrogen composition and stable isotope as potential indicators of source and fate of organic matter in the salt marsh of the Changjiang Estuary, China. Chemosphere 65, 310–317. https://doi.org/10.1016/j.chemosphere.2006.02.026.

Zilius, M., Giordani, G., Petkuviene, J., Lubiene, I., Ruginis, T., Bartoli, M., 2015. Phosphorus mobility under short-term anoxic conditions in two shallow eutrophic coastal systems (Curonian and Sacca di Goro lagoons). Estuar. Coast Shelf Sci. 164, 134–146. https://doi.org/10.1016/j.ecss.2015.07.004.

Zuur, A.F., Ieno, E.N., Elphick, C.S., 2010. A protocol for data exploration to avoid common statistical problems. Methods Ecol. Evol. 1, 3–14. https://doi.org/10.1111/j.2041-210x.2009.00001.x.

Glossary

F_i =: Net fluxes of O_2, DIP, NH_4^+, SiO_2 measured in dark and light conditions (mmol m^{-2} h^{-1})
C_o =: Concentrations of O_2, DIP, NH_4^+, SiO_2 at time zero of incubation (mmol L^{-1})
C_f =: Concentrations of O_2, DIP, NH_4^+, SiO_2 at the end of incubation (mmol L^{-1})
V =: Volume of water column in the core (L)
A =: Area of sediment surface in the core (m^2)
t =: Incubation time (h)
O_{2Bc}, DIP_{Bc}, NH_{4Bc}^+ and SiO_{2Bc} =: Daily O_2 and nutrient fluxes in the benthic compartment (mmol m^{-2} d^{-1})
O_{2Pg}, DIP_{Pg}, NH_{4Pg}^+ and SiO_{2Pg} =: Daily O_2 and nutrient fluxes in the pelagic compartment (mmol m^{-2} d^{-1})
DIP_{WC}, NH_{4WC}^+, NO_{3WC}^-, DIN_{WC}, $SiO_{2\ WC}$ =: Nutrient concentrations in the water column (μM)
DO_{WC} =: Concentration of O_2 in the water column (mg O_2 L^{-1})
$Chl\text{-}a_{WC}$ =: Concentration of chlorophyll-a in the water column (mg Chl-a m^{-3})
$aD\%O\ (abs|100\text{-}\%O_2|)$ =: the absolute value of the difference between measured and 100 % dissolved O_2 saturation (%)
k and m =: Scalar values introduced to adjust the lower limit value and the range of the TRIX
$TRIX$ =: trophic index of the water column
NH_{4pw}^+, DIP_{pw}, SiO_{2pw} =: Nutrient concentrations in the pore water (μM)
$Mn_{pw}(II)$ and $Fe_{pw}(II)$ =: Reduced iron and manganese concentrations in the pore water (μM)
H_2S_{pw} =: Free sulphides concentration in the pore water, $\sum H_2S + HS^- + S^{2-}$ (μM)
SO_{4pw}^{2-} =: Sulfate concentration in pore water (μM)
Fe_{tot} =: Total iron pool in solid-phase in sediment (μmol ml^{-1})
$\%Fe(III)_{sed}$ =: Proportion of oxidize iron pool in solid-phase in the sediment (%)
$Chl\text{-}a_{sed}$ =: Concentration of chlorophyll-a from the upper 1 cm of superficial sediment (μg L^{-1})
TOC and TN =: Total organic carbon and nitrogen pool in the sediment (%)
$\delta^{13}C$ and $\delta^{15}N$ =: Carbon and nitrogen isotopic composition in the sediment (‰)
$\delta^{13}C_{marine}$ =: The $\delta^{13}C$ of marine end member of two-end – member mixing model (‰)
$\delta^{13}C_{terrestrial}$ is the: $\delta^{13}C$ of terrestrial end member of two-end – member mixing model (‰)
$\delta^{13}Corg$ is the: measured value in sediment samples (‰)
TOC_{Terr} =: Contribution of terrestrial organic carbon to TOC calculated using the two-end-member mixing model (%)
TOC_{Marine} =: Contribution of marine organic carbon to the TOC (%)
T_{Anoxic} =: The timescale to anoxia occurrence or the onset of anoxia (d)
T_{NH4} and T_{DIP} =: Benthic turnover times for NH_4^+ and DIP to water column (d)
O_{2in} =: Initial O_2 availability in each station (mmol O_2 m^{-2})
$NetO_2D$ =: Daily O_2 net consumption rate (mmol O_2 m^{-2} d^{-1})
O_{2Alg} =: Daily O_2 flux measured for seaweeds (*Ulva* sp., and *Gracilaria* sp.) in water incubations (mmol O_2 m^{-2} d^{-1})
R_{Air} =: Reaeration coefficient (mmol O_2 m^{-2} d^{-1})
k_1 =: O_2 exchange coefficient between the water surface and the atmosphere (m h^{-1})
C_{WC} =: DO concentration in the water column (mmol O_2 L^{-1})
C_{Sat} =: DO concentration at saturation (mmol O_2 L^{-1})
Sc =: The Schmidt number to determine the physical air-water O_2 exchange, dimensionless
k_{600} =: Coefficient of gas exchange with a Schmidt number = 600 (m h^{-1})
K_V =: Vertical turbulent diffusion coefficient (m^2 s^{-1})
U_{10} =: Average wind speed at 10 m obtained in each station by the hydrodynamic model SHYFEM (m s^{-1})
T_f =: Flushing time estimated by the hydrodynamic model SHYFEM (d)
T_R =: Residence time (d)
T_V =: Vertical exchange timescale (d)
γ =: nondimensional number that relates the timescale of anoxia occurrence to the water residence time.
γ_V =: nondimensional number that relates the timescale of anoxia occurrence to the vertical exchange timescale